Electronic Supplementary Material (ESI) for Journal of Materials Chemistry C.

Equilibrating the Key Parameters of Thermally Activated Delayed Fluorescence Emitters towards Efficient Red/Near-Infrared OLEDs

Jinming Fan,[a,b] *Yulin Xu,*[a] *Nengquan Li,*[a] *Jingsheng Miao,*[a] *Changjiang Zhou,*[c] *Tengxiao Liu,*[d] *Minrong Zhu,*[a] and *Xiaojun Yin* [a,*]

[a]Shenzhen Key Laboratory of New Information Display and Storage Materials, College of Materials Science and Engineering, Shenzhen University, Shenzhen 518060, People's Republic of China.

[b]College of Physics and Optoelectronic Engineering, Shenzhen University, Shenzhen 518060, People's Republic of China.

[c]College of Chemical Engineering, Zhejiang University of Technology, Hangzhou, 310014, PR China.

[d]College of Chemistry and Environmental Science, Wuhan Institute of Bioengineering, Wuhan, 430415, People's Republic of China.

E-Mail: xiaojunyin@szu.edu.cn

Experimental Section

^{1}H NMR and ^{13}C NMR spectra were recorded on Bruker AV 400M, 500M, 600M NMR spectrometer at room temperature using $CDCl_3$, DMSO-d_6 as solvent, and referenced externally to $SiMe_4$. The multiplicities of the signals are indicated as "*s*", "*d*", "*t*" or "*m*", which stand for singlet, doublet, triplet, and multiplet, respectively. High-resolution mass spectra (HRMS) were recorded on a Bruker MAXIS spectrometer in an APCI positive mode. Thermogravimetric analysis (TGA) was recorded on a TA Q50 instrument under nitrogen atmosphere at a heating rate of 10 ℃/min from 25 to 800 ℃. The temperature of degradation (T_d) was correlated to a 5% weight loss. Differential Scanning Calorimetry (DSC) were carried out on a TA Q200. The glass transition temperature (T_g) was determined from the second heating scan at a heating rate of 10 ℃/min from 25 to 400 ℃. Cyclic voltammetry (CV) measurements were carried out on a CHI600 electrochemical analyzer (Chenhua, China) at room temperature, with a conventional three-electrode system consisting of a glassy carbon working electrode, a platinum wire auxiliary electrode, and an Ag/AgCl standard electrode was used as the reference electrode. The supporting electrolyte was 0.1 M tetrabutylammonium hexafluorophosphate (n-Bu_4NPF_6) in anhydrous dichloromethane solution, and ferrocene was added as an internal standard in the whole measurement. UV-Vis spectra in solution were recorded on a UV-3100 spectrophotometer at room temperature. Room-temperature photoluminescence spectra and phosphorescence spectra were measured on a Hitachi F-7000 fluorescence spectrophotometer with xenon lamp as the light source. The absolute fluorescence quantum yields (PLQY) were measured on a Quantaurus-QY measurement system (C9920-02, Hamamatsu Photonics) equipped with a calibrated integrating sphere. During the PLQY measurements, the integrating sphere was purged with pure and dry argon to maintain an inert environment. The lifetimes of fluorescence and delayed fluorescence were performed on PicoQuant Fluotime300.

Theoretical Calculations Method.

Density functional theory (DFT) calculations of the geometrical and electronic properties of the three emitters at ground-states were performed by using Gaussian 16 software package at the B3LYP/def2-SVP level including Grimme's dispersion correction. Time-dependent DFT (TD-DFT) calculations with PBE0 functional and def2-SVP basis set were then performed to further study the properties at excited states. All calculations were performed in the gas phase, and visualized using GaussView 6.0. The wave function analysis was carried out by using Multiwfn 3.8.[1]

Analysis of Rate Constants:

The rate constants of radiative decay ($k_{r,s}$) and nonradiative decay ($k_{nr,s}$) from S_1 to S_0 states, the rate constants of intersystem crossing (k_{ISC}) and reverse intersystem crossing (k_{RISC}) were calculated from the following six equations:

$$k_p = 1/\tau_p \quad \textbf{(1)}$$

$$k_d = 1/\tau_d \quad \textbf{(2)}$$

$$k_{r,s} = \Phi_p k_p + \Phi_d k_d \approx \Phi_p k_p \quad \textbf{(3)}$$

$$k_{nr,s} = [(1-\Phi_{PL}) / \Phi_{PL}]\, k_{r,S} \quad \textbf{(4)}$$

$$k_{ISC} = k_p - k_{r,S} - k_{nr,S} \quad \textbf{(5)}$$

$$k_{RISC} = (k_p k_d \Phi_d)/(k_{ISC} \Phi_p) \quad \textbf{(6)}$$

Where τ_p and τ_d represent the prompt and decay fluorescence lifetime, which determined from transient PL spectra. The *kp* and *kd* represent the decay rate constants for prompt and delayed fluorescence, respectively. Φ_p and Φ_d indicate prompt and delayed fluorescence components and can be distinguished from the total Φ_{PL} by comparing the integrated intensities of prompt and delayed components in the transient PL spectra.

Synthesis of Materials.

All reagents and chemicals (at least analytical grade) were purchased from commercial sources and used without further purification. Solvents were all dried and degassed using the Grubbs-type solvent purification system. The **dpTPAAP** was synthesized according to the previously literatures [2]. Schlenk technology was strictly performed under argon conditions in all reactions. Air- and moisture-sensitive liquids and solutions were transferred via syringes. The final products were firstly purified by column chromatography, and then further refined by temperature-gradient vacuum sublimation (**Scheme S1**).

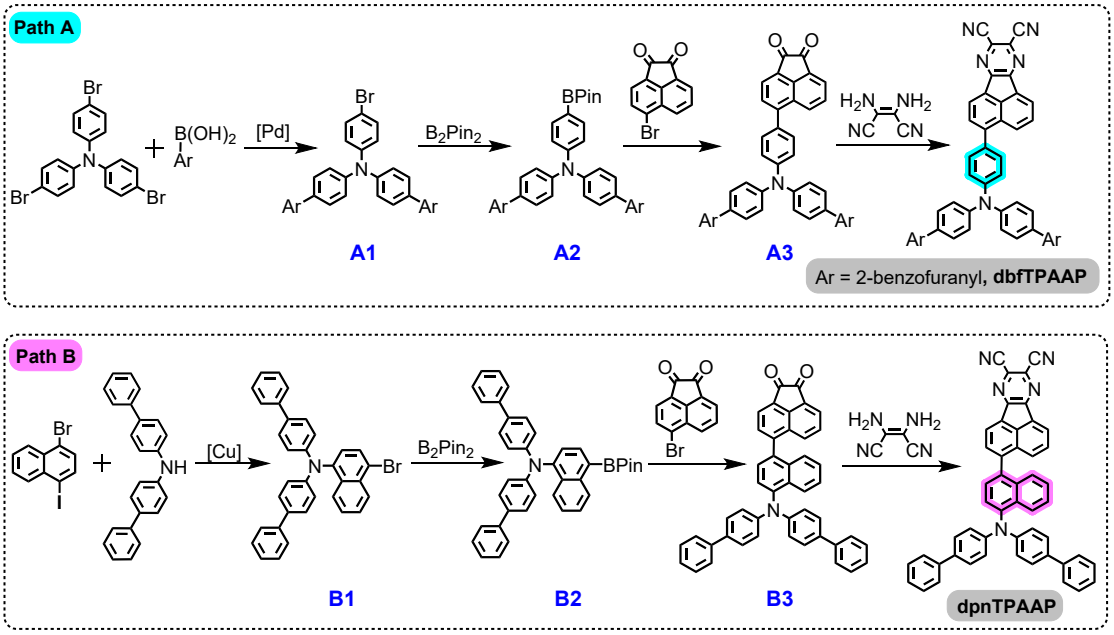

Scheme S1. Synthesis routes of the two red TADF emitters.

General procedure for the synthesis of dbfTPAAP (Path A).

Synthesis of 4-(benzofuran-2-yl)-N-(4-(benzofuran-2-yl)phenyl)-N-(4-bromophenyl)aniline (A1)

The mixture of tris(4-bromophenyl)amine (1eq, 4 mmol, 1.93g), benzofuran-2-boronic acid (3 eq, 12 mmol, 1.94g), $Pd(PPh_3)_4$ (4 %, 0.16 mmol, 0.185 g), K_2CO_3 (4 eq, 16 mmol, 2.2 g) was dissolved in a mixed solvent composed of toluene/THF/H_2O

(5/5/1, 20/20/4 ml). The reaction mixture was allowed to stir at 80 °C for 12 h under Ar. Then the reaction mixture was cooled at room temperature and filtered through Celite. Filtrate was concentrated under reduced pressure, the residue was dissolved in CH_2Cl_2 (100 mL × 3), washed with water and dried over Na_2SO_4. Combined organic layers were evaporated under reduced pressure, and the residue was purified by column chromatography on silica [CH_2Cl_2/Petroleum ether = 1/20 ~1/10] to provide pure **A1** (white solid, 78%, 1.73g).

Synthesis of 4-(benzofuran-2-yl)-N-(4-(benzofuran-2-yl)phenyl)-N-(4-(4,4,5,5-tetramethyl-1,3,2-dioxaborolan-2-yl)phenyl)aniline (A2)

The mixture of **A1** (1eq, 2 mmol, 1.11g), bis(pinacolato)diboron (3 eq, 6 mmol, 1.53g), Pd(dppf)Cl_2 (5 %, 0.1 mmol, 0.073 g), KOAc (5 eq, 10 mmol, 1 g) was dissolved in a mixed solvent composed of dioxane (30 ml). The reaction mixture was allowed to stir at 110 °C for 12 h under Ar. Then the reaction mixture was cooled at room temperature and filtered through Celite. Filtrate was concentrated under reduced pressure, the residue was dissolved in CH_2Cl_2 (30 mL × 3), washed with water and dried over Na_2SO_4. Combined organic layers were evaporated under reduced pressure, and the residue was purified by column chromatography on silica [CH_2Cl_2/Petroleum ether = 1/3 ~1/1] to provide pure **A2** (yellow solid, 95%, 1.15g).

Synthesis of 5-(4-(bis(4-(benzofuran-2-yl)phenyl)amino)phenyl) acenaphthy-lene-1,2-dione (A3)

The mixture of **A2** (1eq, 2 mmol, 1.2g), 5-bromoacenaphthylene-1,2-dione (1 eq, 2 mmol, 0.53g), Pd(PPh_3)$_4$ (5 %, 0.1 mmol, 0.12 g), K_2CO_3 (5 eq, 10 mmol, 1.4 g) was dissolved in a mixed solvent composed of dioxane/H_2O (10/10 ml). The reaction mixture was allowed to stir at 110 °C for 12 h under Ar. Then the reaction mixture was cooled at room temperature and filtered through Celite. Filtrate was concentrated under reduced pressure, the residue was dissolved in CH_2Cl_2 (30 mL × 3), washed with water and dried over Na_2SO_4. Combined organic layers were evaporated under reduced pressure, and the residue was purified by column chromatography on silica [CH_2Cl_2/Petroleum ether = 1/5 ~1/1] to provide pure **A3** (red solid, 76%, 1g).

Synthesis of 3-(4-(bis(4-(benzofuran-2-yl)phenyl)amino)phenyl)acenaphtho[1,2-b] pyrazine -8,9-dicarbonitrile (dbfTPAAP)

The mixture of **A3** (1eq, 2 mmol, 1.3g) and 2,3-diaminomaleonitrile (1 eq, 2 mmol, 0.22g) was dissolved in AcOH (20 ml). The reaction mixture was allowed to stir at 120 °C for 36 h under Ar. Then the reaction mixture was cooled at room temperature and concentrated under reduced pressure, the residue was dissolved in CH_2Cl_2 (30 mL × 3), washed with water and dried over Na_2SO_4. Combined organic layers were evaporated under reduced pressure, and the residue was purified by column chromatography on silica [CH_2Cl_2/Petroleum ether = 1/3 ~ CH_2Cl_2] to provide pure **dbfTPAAP** (black solid, 67%, 0.98g).

General procedure for the synthesis of dpnTPAAP (Path B).

Synthesis of N,N-di([1,1'-biphenyl]-4-yl)-5-bromonaphthalen-1-amine (B1)

The mixture of 1-bromo-4-iodonaphthalene (1eq, 5 mmol, 1.65g), bis(4-biphenylyl)amine (1 eq, 5 mmol, 1.60g), CuI (1 %, 0.05 mmol, 0.01 g), trans-1,2-cyclohexanediamine (10 %, 0.5 mmol, 0.06 g) and *t*-BuOK (1.5 eq, 7.5 mmol, 0.84 g) was dissolved in a mixed solvent composed of dioxane (15 ml). The reaction mixture was allowed to stir at 100 °C for 24 h under Ar. Then the reaction mixture was cooled at room temperature and filtered through Celite. Filtrate was concentrated under reduced pressure, the residue was dissolved in CH_2Cl_2 (100 mL × 3), washed with water and dried over Na_2SO_4. Combined organic layers were evaporated under reduced pressure, and the residue was purified by column chromatography on silica [CH_2Cl_2/Petroleum ether = 1/20 ~1/10] to provide pure **B1** (white solid, 86%, 2.26g).

Synthesis of N,N-di([1,1'-biphenyl]-4-yl)-5-(4,4,5,5-tetramethyl-1,3,2-dioxaborolan-2-yl)naphthalen-1-amine (B2)

The mixture of **B1** (1eq, 2 mmol, 1.05g), bis(pinacolato)diboron (3 eq, 6 mmol, 1.53g), Pd(dppf)Cl_2 (5 %, 0.1 mmol, 0.073 g), KOAc (5 eq, 10 mmol, 1 g) was

dissolved in a mixed solvent composed of dioxane (30 ml). The reaction mixture was allowed to stir at 110 °C for 12 h under Ar. Then the reaction mixture was cooled at room temperature and filtered through Celite. Filtrate was concentrated under reduced pressure, the residue was dissolved in CH_2Cl_2 (30 mL × 3), washed with water and dried over Na2SO4. Combined organic layers were evaporated under reduced pressure, and the residue was purified by column chromatography on silica [CH_2Cl_2/Petroleum ether = 1/10 ~1/5] to provide pure **B2** (yellow solid, 77%, 0.88g).

Synthesis of 5-(5-(di([1,1'-biphenyl]-4-yl)amino)naphthalen-1-yl)acenaphthylene-1,2-dione (B3)

The mixture of **B2** (1eq, 2 mmol, 1.15g), 5-bromoacenaphthylene-1,2-dione (1 eq, 2 mmol, 0.53g), $Pd(PPh_3)_4$ (5 %, 0.1 mmol, 0.12 g), K_2CO_3 (5 eq, 10 mmol, 1.4 g) was dissolved in a mixed solvent composed of dioxane/H_2O (10/10 ml). The reaction mixture was allowed to stir at 110 °C for 12 h under Ar. Then the reaction mixture was cooled at room temperature and filtered through Celite. Filtrate was concentrated under reduced pressure, the residue was dissolved in CH_2Cl_2 (3 mL × 3), washed with water and dried over Na_2SO_4. Combined organic layers were evaporated under reduced pressure, and the residue was purified by column chromatography on silica [CH_2Cl_2/Petroleum ether = 1/1 ~ CH_2Cl_2] to provide pure **B3** (red solid, 56%, 0.71g).

Synthesis of 3-(5-(di([1,1'-biphenyl]-4-yl)amino)naphthalen-1-yl)acenaphtho[1,2-b]pyrazine-8,9-dicarbonitrile (dpnTPAAP)

The mixture of **B3** (1eq, 2 mmol, 1.25g) and 2,3-diaminomaleonitrile (1 eq, 2 mmol, 0.22g) was dissolved in AcOH (20 ml). The reaction mixture was allowed to stir at 120 °C for 36 h under Ar. Then the reaction mixture was cooled at room temperature and concentrated under reduced pressure, the residue was dissolved in CH_2Cl_2 (30 mL × 3), washed with water and dried over Na_2SO_4. Combined organic layers were evaporated under reduced pressure, and the residue was purified by column chromatography on silica [CH_2Cl_2/Petroleum ether = 1/3 ~ CH_2Cl_2] to provide pure **dpnTPAAP** (black solid, 58%, 0.81g).

NMR and HRMS data:

4-(Benzofuran-2-yl)-N-(4-(benzofuran-2-yl)phenyl)-N-(4-bromophenyl)aniline (A1)

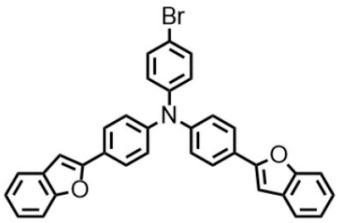

^{1}H NMR (500 MHz, Chloroform-*d*) δ 7.82 – 7.73 (m, 4H), 7.61 – 7.55 (m, 2H), 7.52 (dd, *J* = 7.9, 1.1 Hz, 2H), 7.46 – 7.39 (m, 2H), 7.28 (ddd, *J* = 8.1, 7.2, 1.5 Hz, 2H), 7.23 (td, *J* = 7.4, 1.1 Hz, 2H), 7.21 – 7.14 (m, 4H), 7.08 – 7.02 (m, 2H), 6.95 (d, *J* = 0.9 Hz, 2H). ^{13}C NMR (126 MHz, Chloroform-*d*) δ 155.78, 154.98, 147.28, 146.22, 132.69, 129.52, 126.44, 126.27, 125.58, 124.21, 123.09, 120.88, 116.44, 111.22, 100.70. HRMS (APCI) m/z calcd for. $C_{34}H_{22}BrNO_2$ $[M+H]^+$ 556.0907, found 556.0902.

4-(Benzofuran-2-yl)-N-(4-(benzofuran-2-yl)phenyl)-N-(4-(4,4,5,5-tetramethyl-1,3,2-dioxaborolan-2-yl)phenyl)aniline (A2)

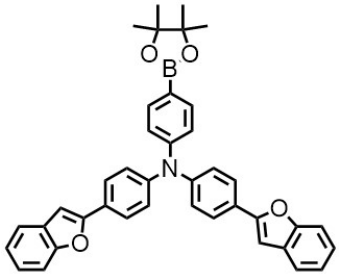

^{1}H NMR (500 MHz, Chloroform-*d*) δ 7.76 (t, *J* = 8.5 Hz, 6H), 7.57 (dd, *J* = 7.5, 1.6 Hz, 2H), 7.54 – 7.47 (m, 2H), 7.29 – 7.25 (m, 3H), 7.25 – 7.13 (m, 8H), 6.95 (s, 2H), 1.36 (s, 12H). ^{13}C NMR (126 MHz, Chloroform-*d*) δ 155.88, 154.98, 149.78, 147.40, 136.25, 129.55, 126.20, 125.61, 124.69, 124.16, 123.35, 123.06, 120.86, 111.21, 100.66, 83.88, 25.02. HRMS (APCI) m/z calcd for. $C_{40}H_{34}BNO_4$ $[M+H]^+$ 604.2654, found 604.2659.

5-(4-(Bis(4-(benzofuran-2-yl)phenyl)amino)phenyl)acenaphthy-lene-1,2-dione (A3)

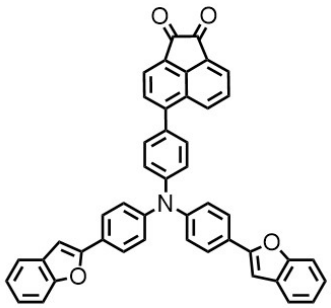

^{1}H NMR (600 MHz, DMSO-d_6) δ 8.44 (d, *J* = 8.6 Hz, 1H), 8.11 (dd, *J* = 11.2, 7.2 Hz, 2H), 7.93 – 7.91 (m, 4H), 7.89 (d, *J* = 7.3 Hz, 1H), 7.70 – 7.67 (m, 2H), 7.65 – 7.59 (m, 5H), 7.35 – 7.33 (m, 3H), 7.30 – 7.24 (m, 9H). ^{13}C NMR (151 MHz, DMSO-d_6) δ 188.07, 187.21, 155.15, 154.29, 146.94, 130.98, 130.58, 129.44, 129.11, 128.99, 128.77, 128.41, 128.15, 126.34, 124.98, 124.50, 124.45, 124.25, 123.32,

121.52, 121.47, 121.09, 111.11, 101.31. HRMS (APCI) m/z calcd for. $C_{46}H_{27}NO_4$ $[M+H]^+$ 658.2013, found 658.2018.

3-(4-(Bis(4-(benzofuran-2-yl)phenyl)amino)phenyl)acenaphtho[1,2-b]pyrazine-8,9-dicarbonitrile (dbfTPAAP)

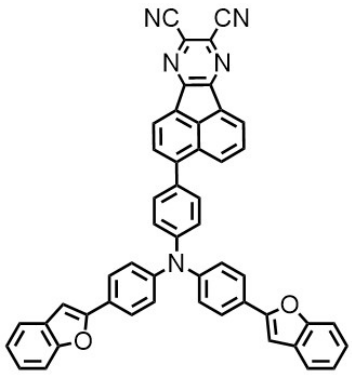

^{1}H NMR (500 MHz, Chloroform-*d*) δ 8.41 (d, *J* = 2.1 Hz, 1H), 8.39 (d, *J* = 6.9 Hz, 2H), 7.89 – 7.81 (m, 2H), 7.73 – 7.69 (m, 4H), 7.55 – 7.49 (m, 2H), 7.47 – 7.45 (m, 2H), 7.41 – 7.38 (m, 2H), 7.32 – 7.28 (m, 2H), 7.22 – 7.20 (m, 3H), 7.15 (dtd, *J* = 14.8, 7.7, 1.3 Hz, 5H), 6.84 (d, *J* = 0.9 Hz, 2H). ^{13}C NMR (126 MHz, Chloroform-*d*) δ 155.60, 154.93, 147.14, 146.42, 132.55, 132.15, 131.58, 129.81, 129.45, 129.41, 129.37, 128.76, 127.16, 126.33, 126.12, 126.01, 124.91, 124.86, 124.33, 124.04, 123.15, 120.92, 111.20, 100.87. HRMS (APCI) m/z calcd for. $C_{50}H_{27}N_5O_2$ $[M+H]^+$ 730.2238, found 730.2227. Elemental analysis (%) calcd for $C_{50}H_{27}N_5O_2$: C 82.29, H 3.73, N 9.60; found: C 82.60, H 4.12, N 9.16.

N,N-Di([1,1'-biphenyl]-4-yl)-5-bromonaphthalen-1-amine (B1)

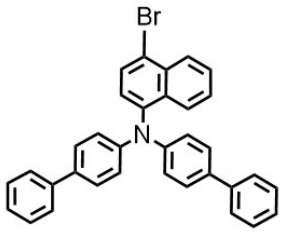

^{1}H NMR (500 MHz, Chloroform-*d*) δ 8.36 – 8.27 (m, 1H), 8.10 – 7.99 (m, 1H), 7.82 (d, *J* = 8.0 Hz, 1H), 7.61 (ddd, *J* = 8.4, 6.8, 1.2 Hz, 1H), 7.59 – 7.54 (m, 4H), 7.50 – 7.46 (m, 4H), 7.43 (q, *J* = 7.6 Hz, 5H), 7.34 – 7.29 (m, 2H), 7.28 (d, *J* = 7.9 Hz, 1H), 7.17 – 7.11 (m, 4H). ^{13}C NMR (126 MHz, Chloroform-*d*) δ 147.47, 143.47, 140.66, 134.93, 130.58, 128.89, 128.00, 127.96, 127.83, 127.51, 126.96, 126.74, 124.92, 122.29, 120.82. HRMS (APCI) m/z calcd for. $C_{34}H_{24}BrN$ $[M+H]^+$ 526.1165, found 526.1170.

N,N-Di([1,1'-biphenyl]-4-yl)-5-(4,4,5,5-tetramethyl-1,3,2-dioxaborolan-2-yl)naphthalen-1-amine (B2)

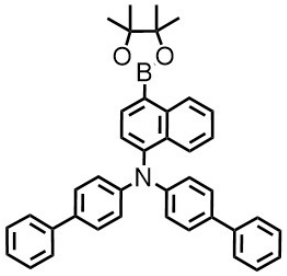

^{1}H NMR (500 MHz, Chloroform-*d*) δ 8.90 – 8.82 (m, 1H), 8.13 (d, *J* = 7.4 Hz, 1H), 8.06 – 8.00 (m, 1H), 7.59 – 7.55 (m, 4H), 7.55 – 7.51 (m, 1H), 7.49 – 7.44 (m, 4H), 7.41 (qd, *J* = 7.3, 1.6 Hz, 6H), 7.30 (td, *J* = 7.3, 1.3 Hz, 2H), 7.17 – 7.11 (m, 4H), 1.46 (s, 12H). ^{13}C NMR (126 MHz, Chloroform-*d*) δ 147.63, 140.78, 136.37, 134.74, 129.14, 128.86, 127.86, 126.87, 126.80, 126.75, 126.37, 126.26, 124.60, 122.39, 83.97, 25.12. HRMS (APCI) m/z calcd for. $C_{40}H_{36}BNO_2$ $[M+H]^+$ 574.2912, found 574.2921.

5-(5-(Di([1,1'-biphenyl]-4-yl)amino)naphthalen-1-yl)acenaphthylene-1,2-dione (B3)

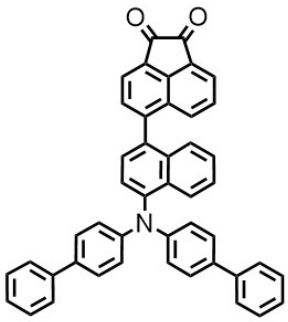

^{1}H NMR (400 MHz, Chloroform-*d*) δ 8.23 (d, *J* = 7.2 Hz, 1H), 8.14 (dd, *J* = 16.0, 7.7 Hz, 2H), 7.93 (dd, *J* = 7.9, 3.0 Hz, 2H), 7.72 (dd, *J* = 8.5, 7.0 Hz, 1H), 7.55 (d, *J* = 8.2 Hz, 6H), 7.50 (d, *J* = 8.5 Hz, 5H), 7.39 (t, *J* = 7.7 Hz, 5H), 7.36 – 7.33 (m, 1H), 7.29 (d, *J* = 7.3 Hz, 2H), 7.21 (d, *J* = 8.3 Hz, 4H). ^{13}C NMR (101 MHz, Chloroform-*d*) δ 147.69, 144.99, 144.65, 140.63, 135.09, 134.05, 132.11, 131.41, 130.52, 128.98, 128.91, 128.66, 128.52, 128.04, 127.13, 127.04, 127.01, 126.73, 126.67, 126.41, 125.13, 122.57, 122.36, 122.07. HRMS (APCI) m/z calcd for. $C_{46}H_{29}NO_2$ $[M+H]^+$ 628.2272, found 628.2271.

3-(5-(Di([1,1'-biphenyl]-4-yl)amino)naphthalen-1-yl)acenaphtho[1,2-b]py-razine-8,9-dicarbonitrile (dpnTPAAP)

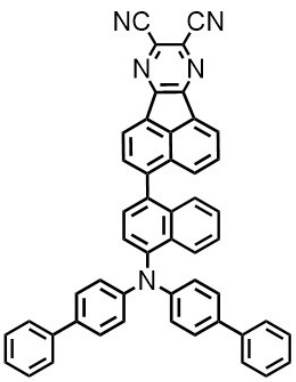

^{1}H NMR (500 MHz, Chloroform-*d*) δ 8.66 (d, *J* = 7.2 Hz, 1H), 8.57 (d, *J* = 7.0 Hz, 1H), 8.19 (d, *J* = 8.5 Hz, 1H), 8.06 (dd, *J* = 14.7, 7.8 Hz, 2H), 7.88 (dd, *J* = 8.4, 7.0 Hz, 1H), 7.63 – 7.56 (m, 7H), 7.56 – 7.52 (m, 4H), 7.43 (t, *J* = 7.7 Hz, 5H), 7.38 (s, 1H), 7.35 – 7.30 (m, 2H), 7.26 – 7.23 (m, 4H). ^{13}C NMR (126 MHz, Chloroform-*d*) δ 154.90, 154.59, 150.07, 147.70, 145.52, 140.66, 135.70, 135.18, 135.15, 134.27, 133.92, 132.43, 131.60, 131.43, 131.38, 130.19, 129.96, 129.91, 129.59,

129.37, 128.94, 128.20, 128.07, 127.12, 127.05, 127.02, 126.77, 126.73, 126.53, 126.18, 125.07, 122.63, 114.37. HRMS (APCI) m/z calcd for. $C_{50}H_{29}N_5$ $[M+H]^+$ 700.2496, found 700.2498. Elemental analysis (%) calcd for $C_{50}H_{29}N_5$: C 85.82, H 4.18, N 10.01; found: C 85.81, H 4.62, N 9.64.

3-(4-(Di([1,1'-biphenyl]-4-yl)amino)phenyl)acenaphtho[1,2-b]pyrazine-8,9-dicarbonitrile (dpTPAAP)

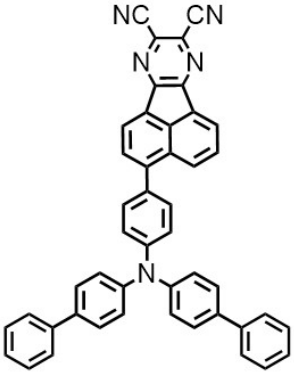

^{1}H NMR (400 MHz, Chloroform-*d*) δ 8.54 (dd, *J* = 7.6, 1.7 Hz, 3H), 8.00 – 7.91 (m, 2H), 7.64 – 7.55 (m, 10H), 7.48 – 7.43 (m, 4H), 7.40 – 7.29 (m, 8H). [1]

NMR and HRMS Spectra.

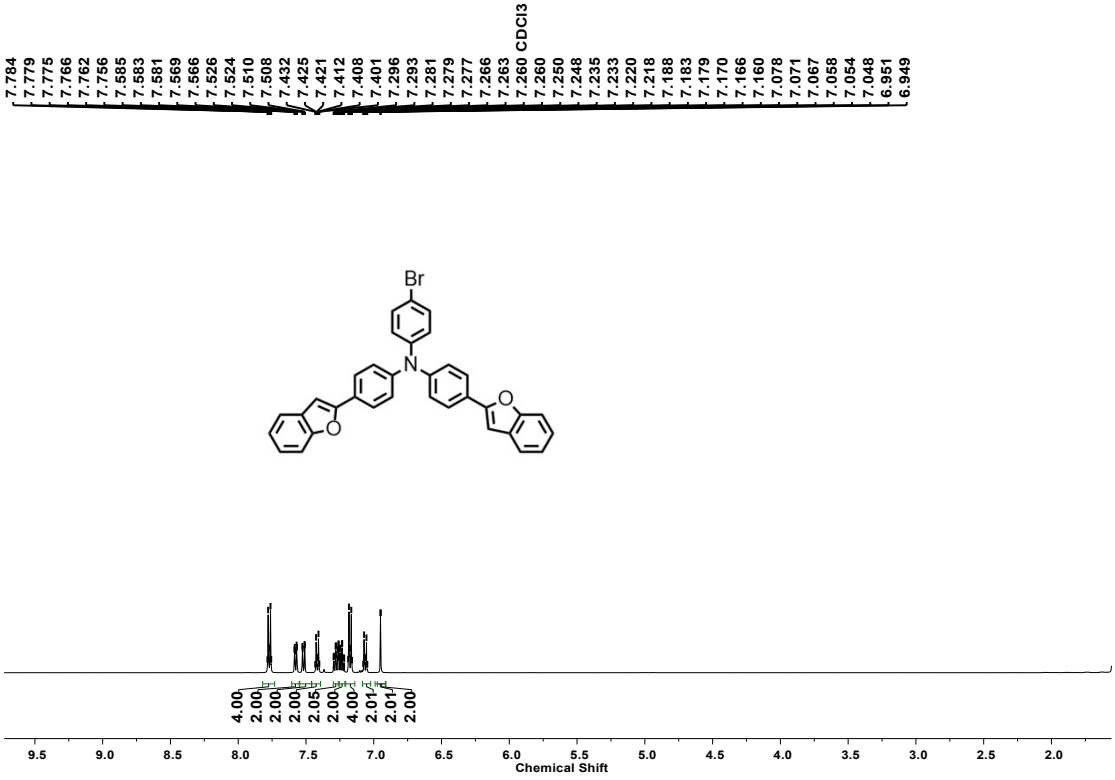

Figure S1. ^{1}H NMR of **A1** in $CDCl_3$.

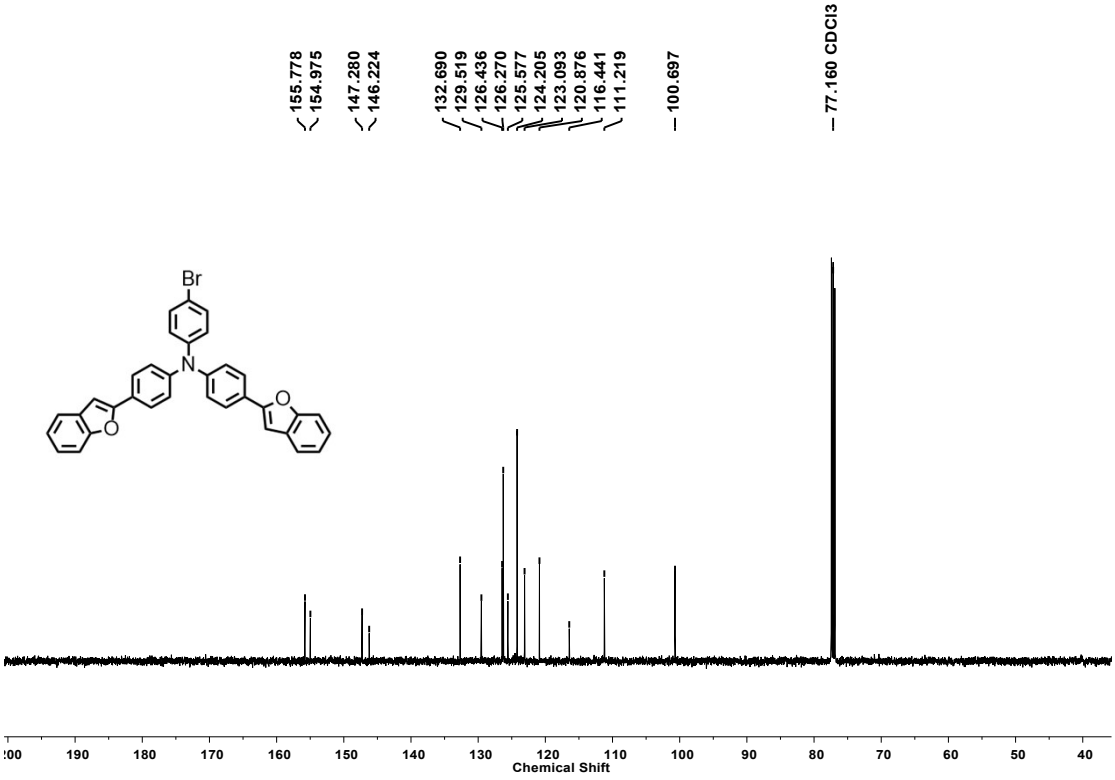

Figure S2. ^{13}C NMR of **A1** in $CDCl_3$.

Acquisition Parameter

Source Type	APCI	Ion Polarity	Positive	Set Nebulizer	1.6 Bar
Focus	Not active	Set Capillary	2000 V	Set Dry Heater	200 °C
Scan Begin	100 m/z	Set End Plate Offset	-500 V	Set Dry Gas	2.5 l/min
Scan End	1100 m/z	Set Collision Cell RF	200.0 Vpp	Set Divert Valve	Waste

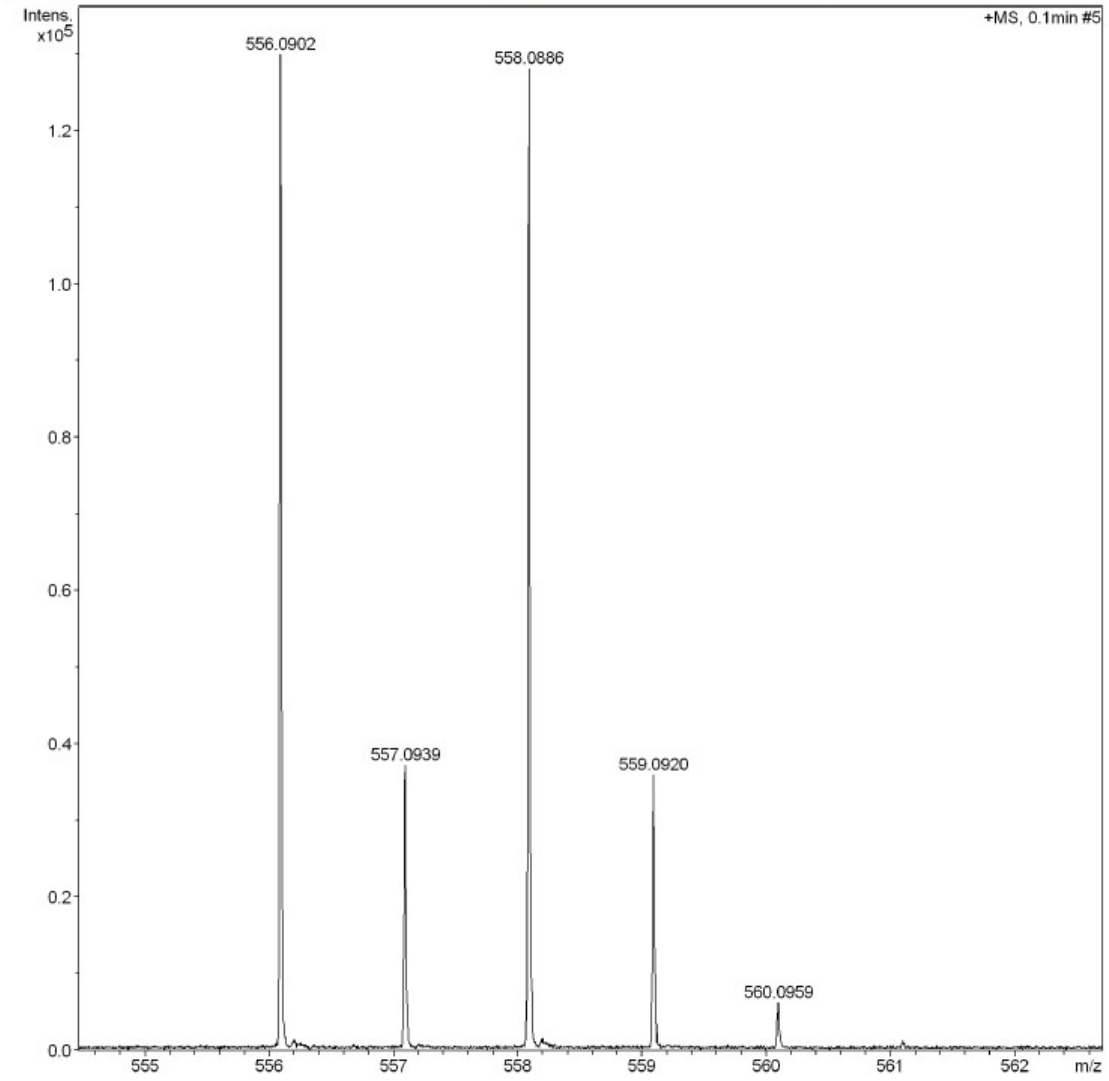

Figure S3. HRMS (APCI) of **A1** in MeOH.

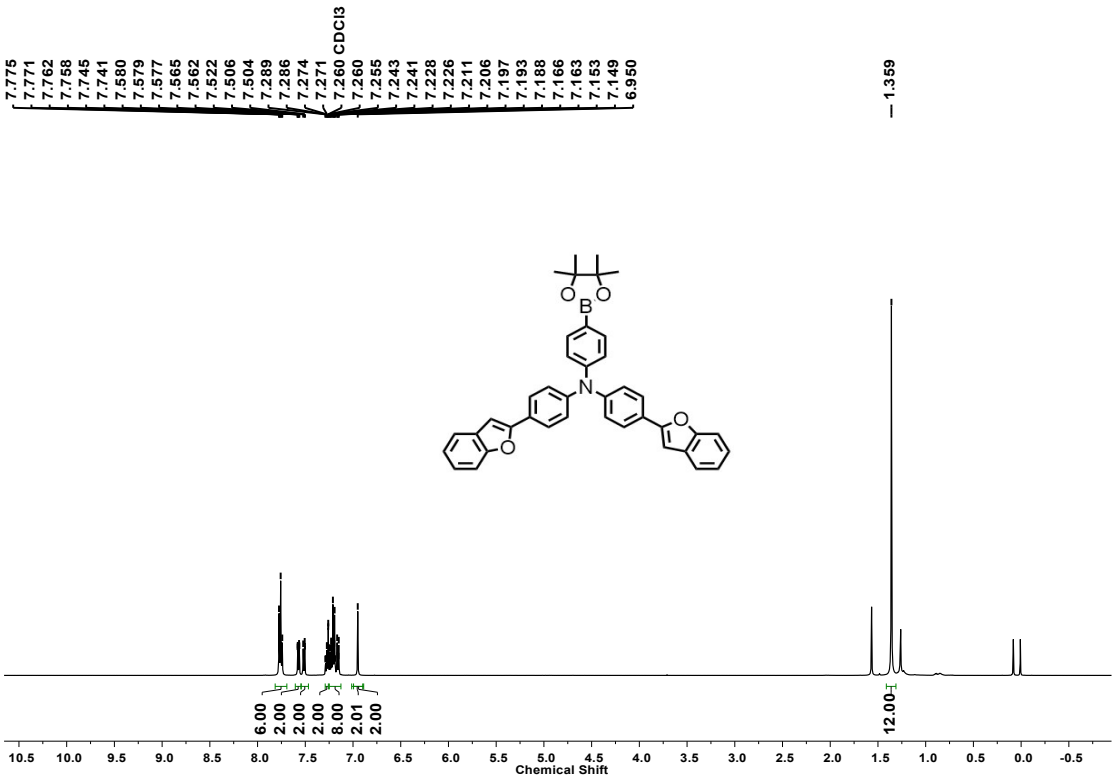

Figure S4. ^{1}H NMR of **A2** in $CDCl_3$.

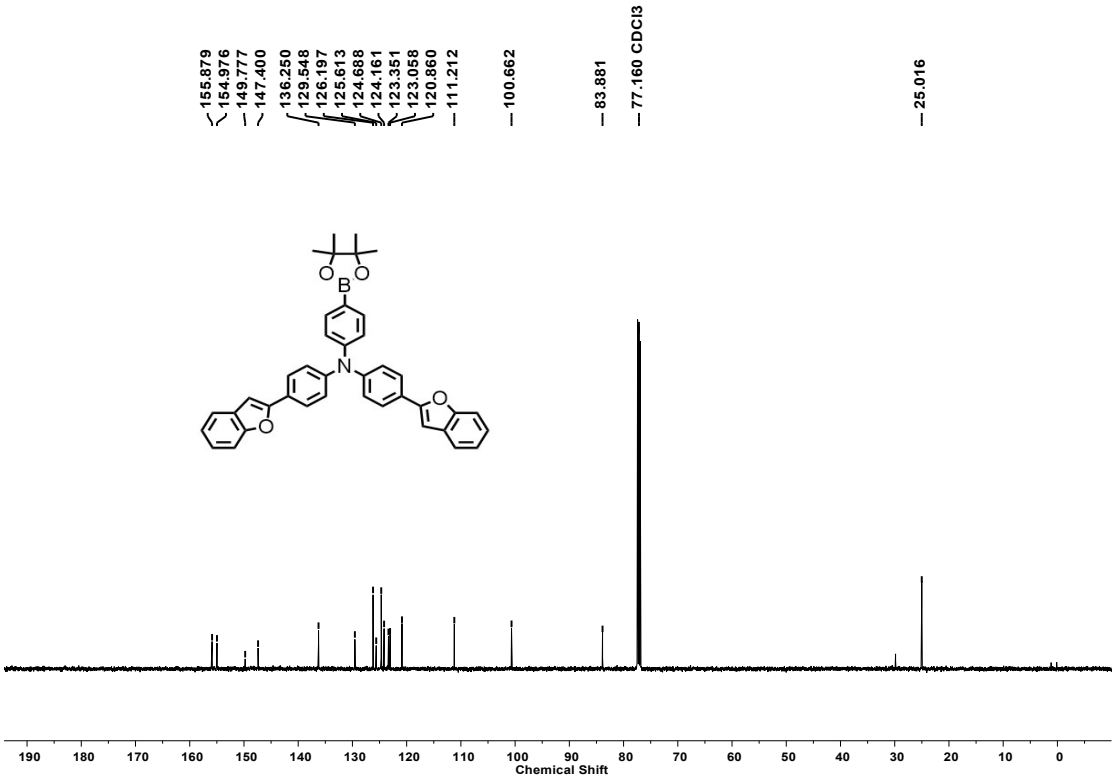

Figure S5. ^{13}C NMR of **A2** in $CDCl_3$.

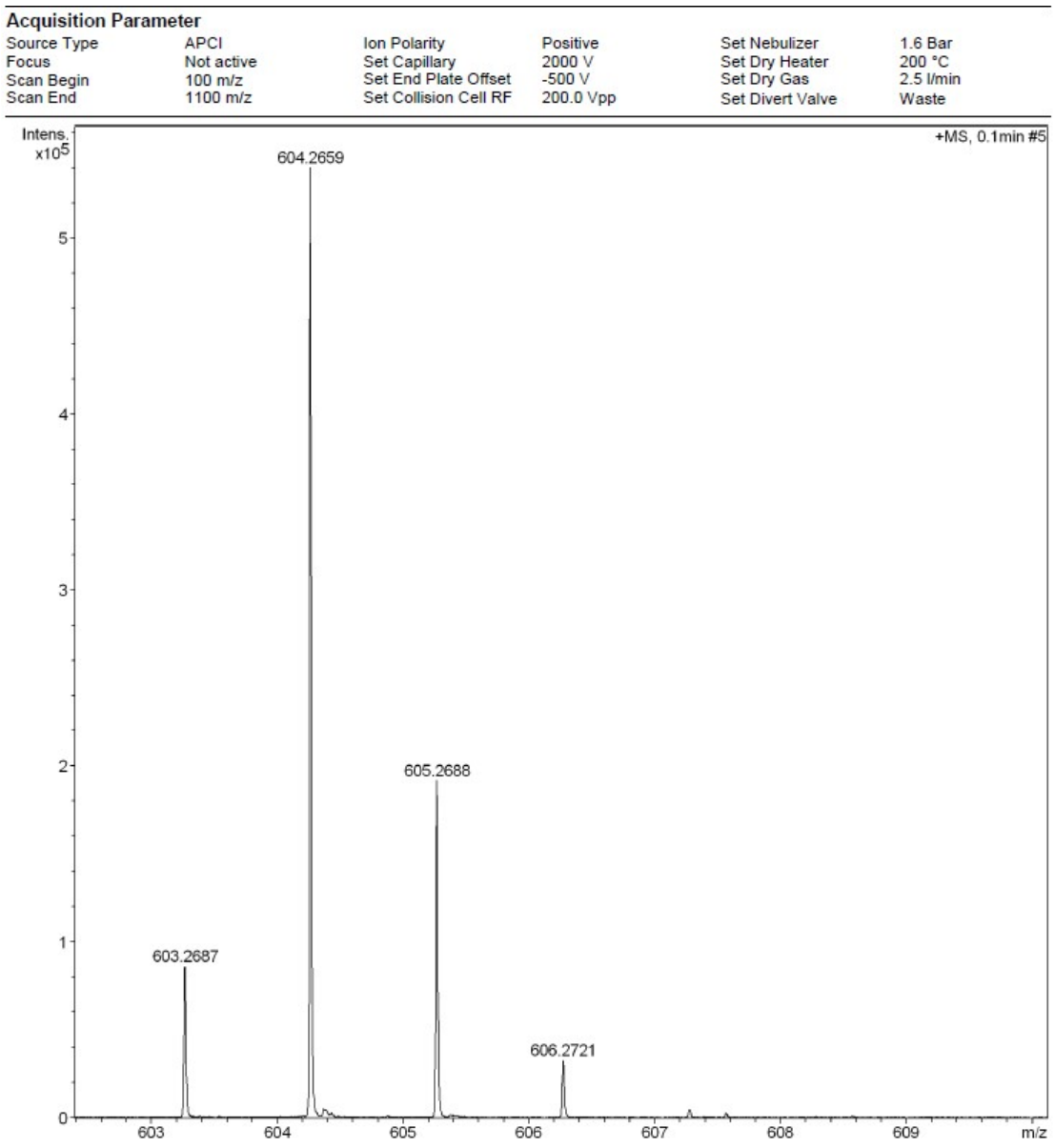

Figure S6. HRMS (APCI) of **A2** in MeOH.

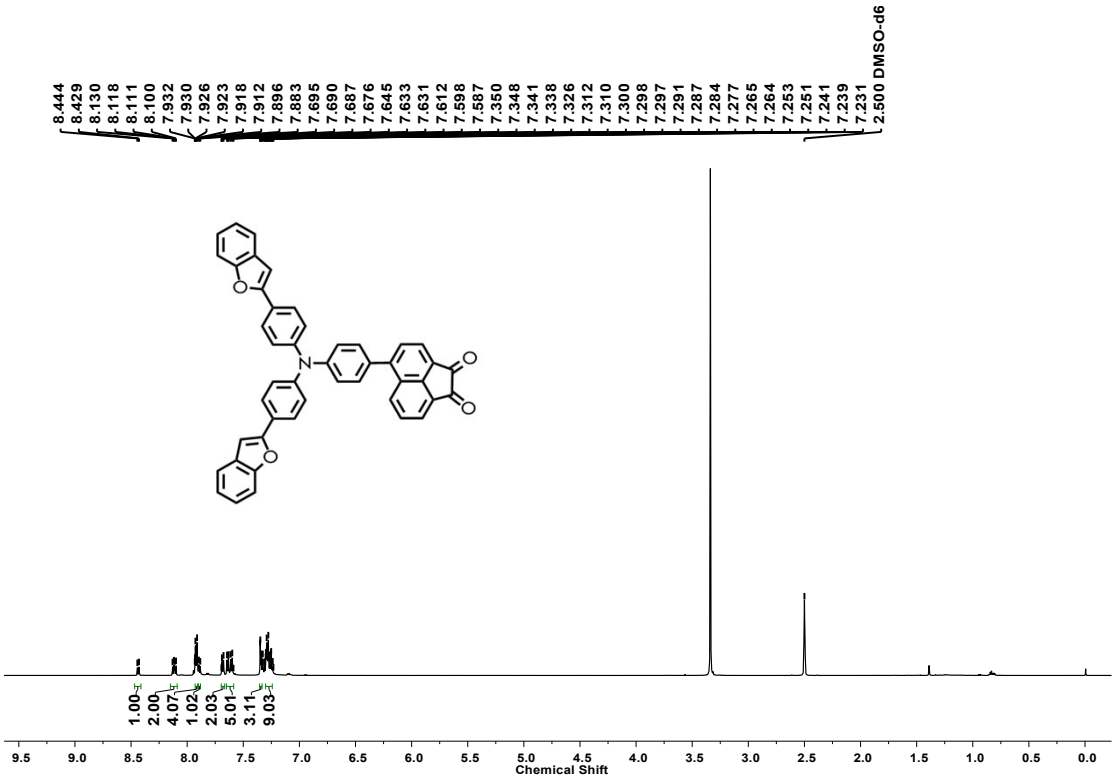

Figure S7. ^{1}H NMR of **A3** in DMSO-d_6.

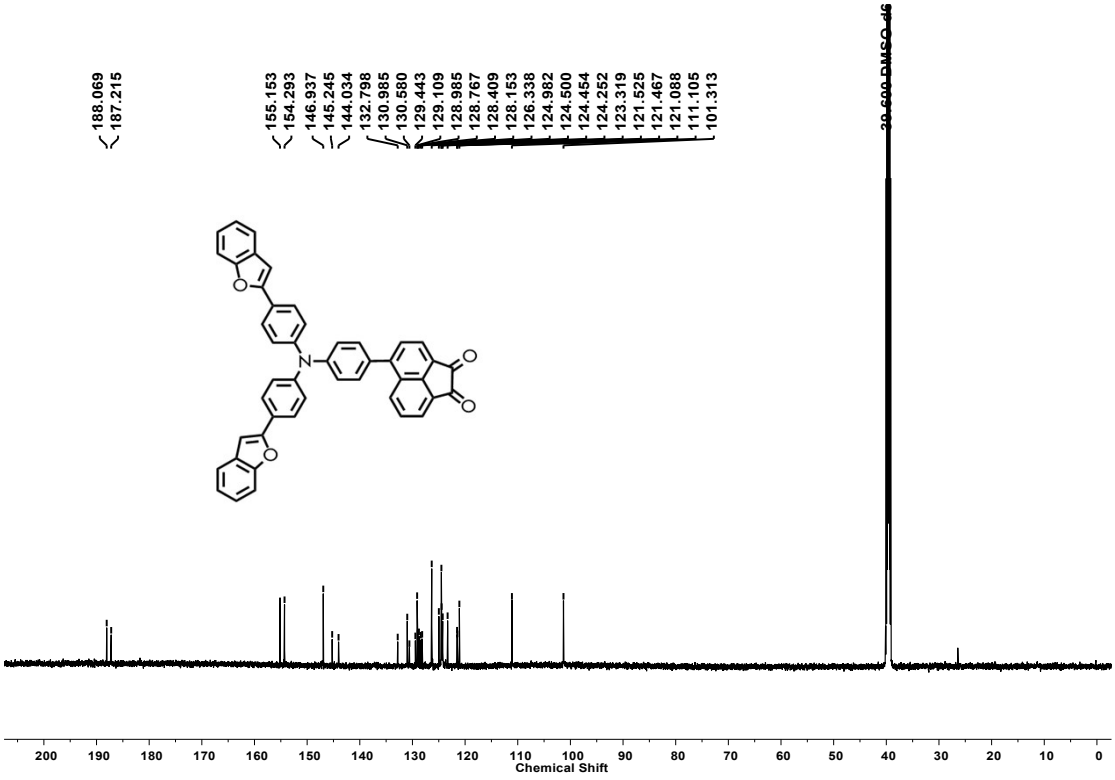

Figure S8. ^{13}C NMR of **A2** in DMSO-d_6.

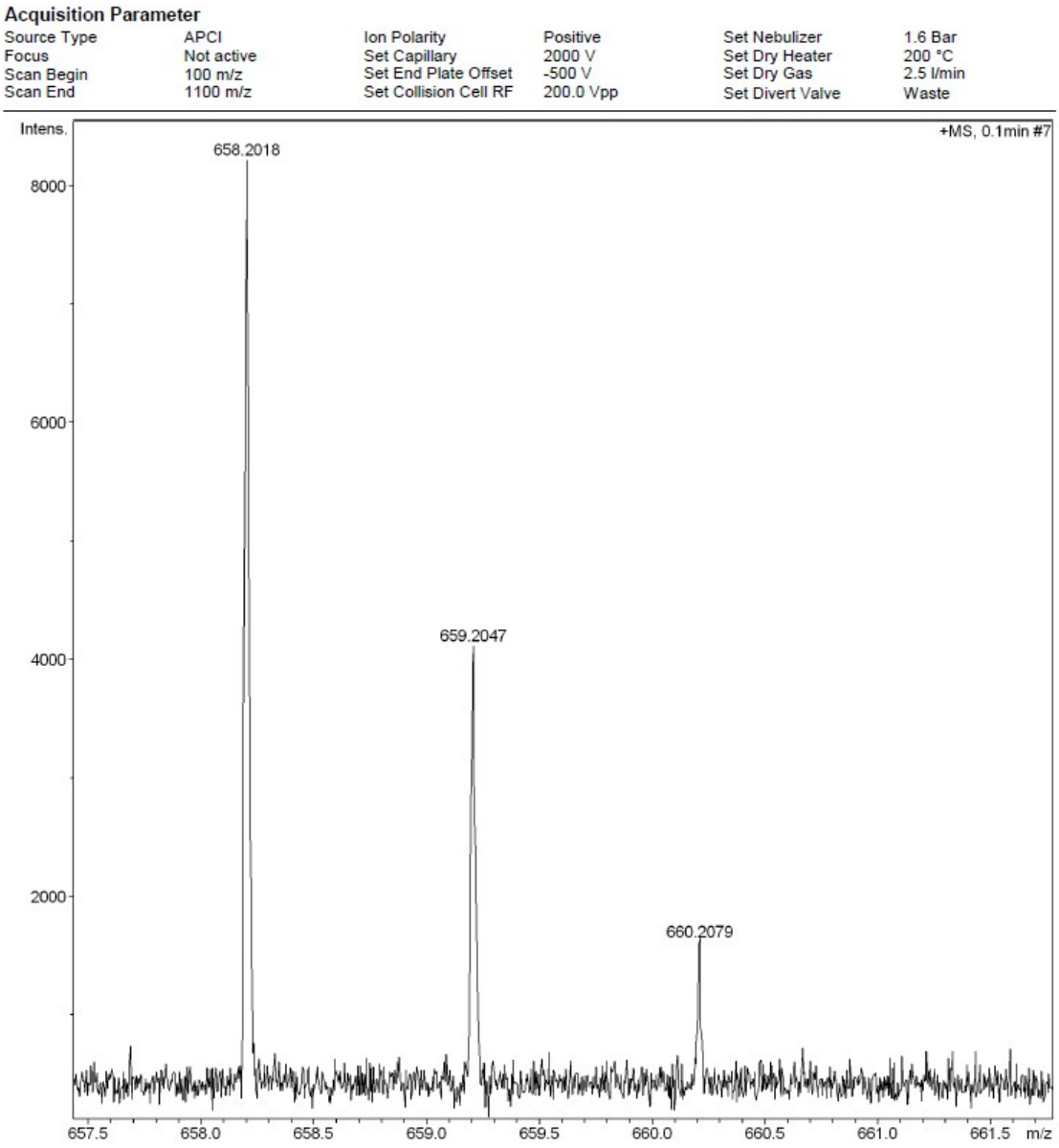

Figure S9. HRMS (APCI) of **A3** in MeOH.

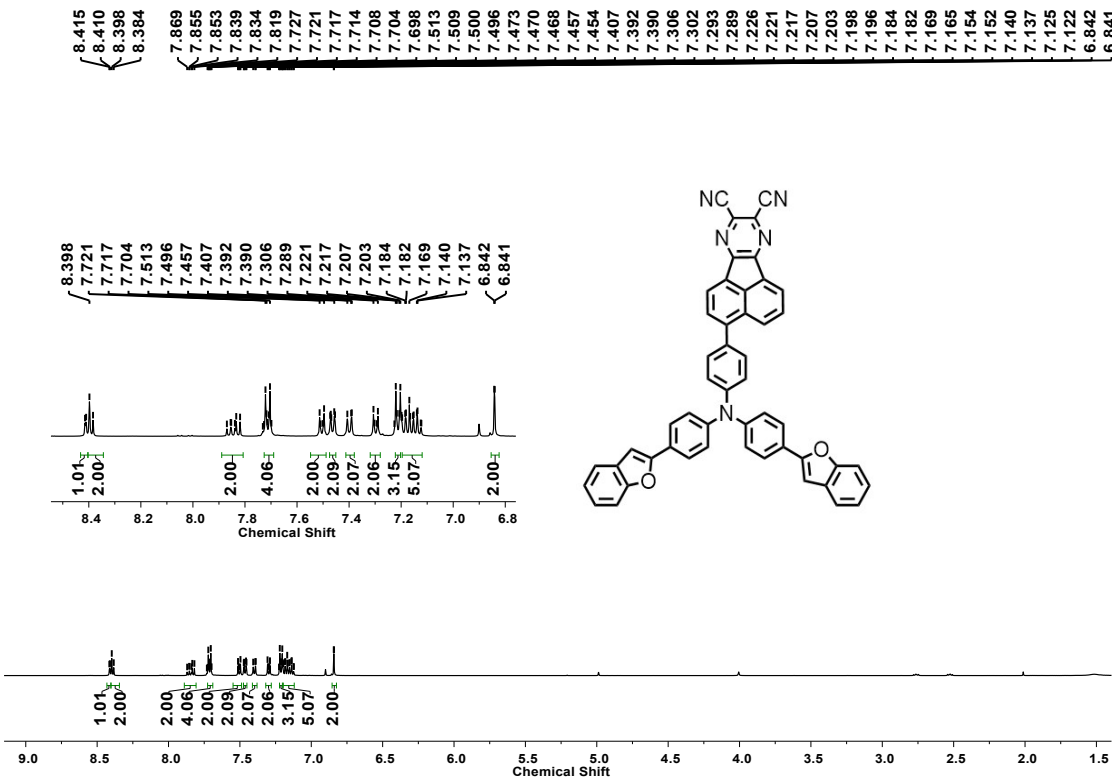

Figure S10. ^{1}H NMR of **dbfTPAAP** in $CDCl_3$.

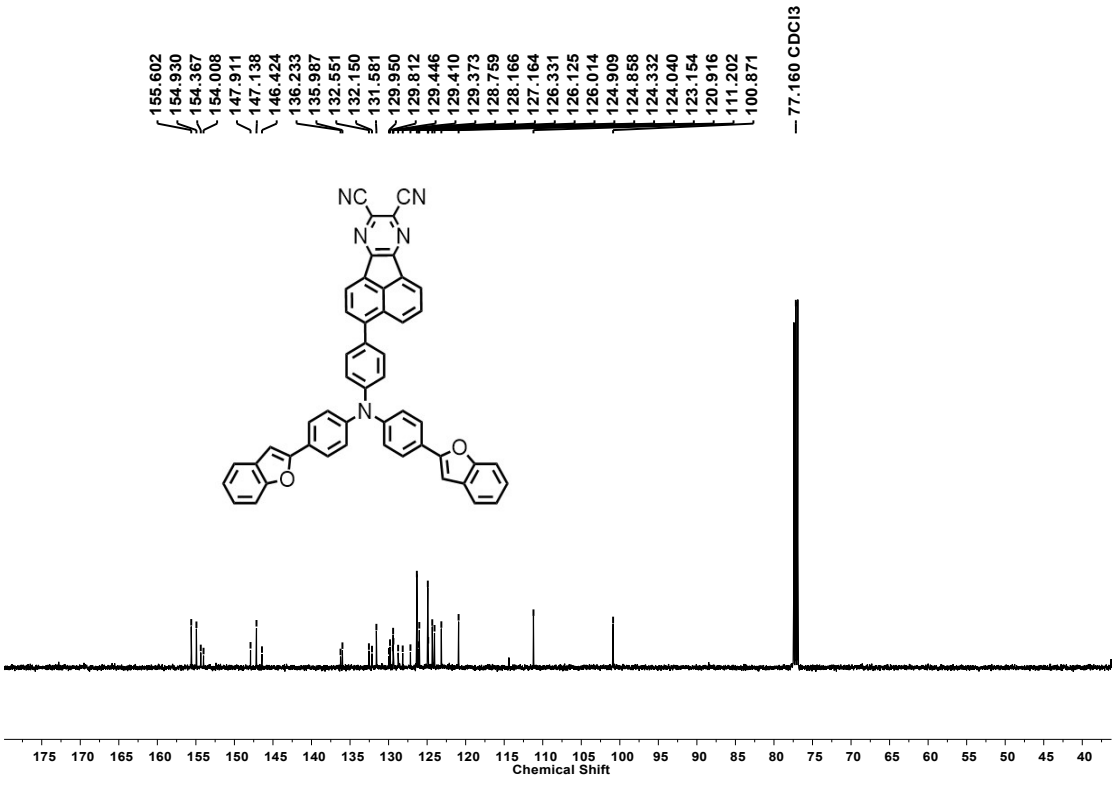

Figure S11. ^{13}C NMR of **dbfTPAAP** in $CDCl_3$.

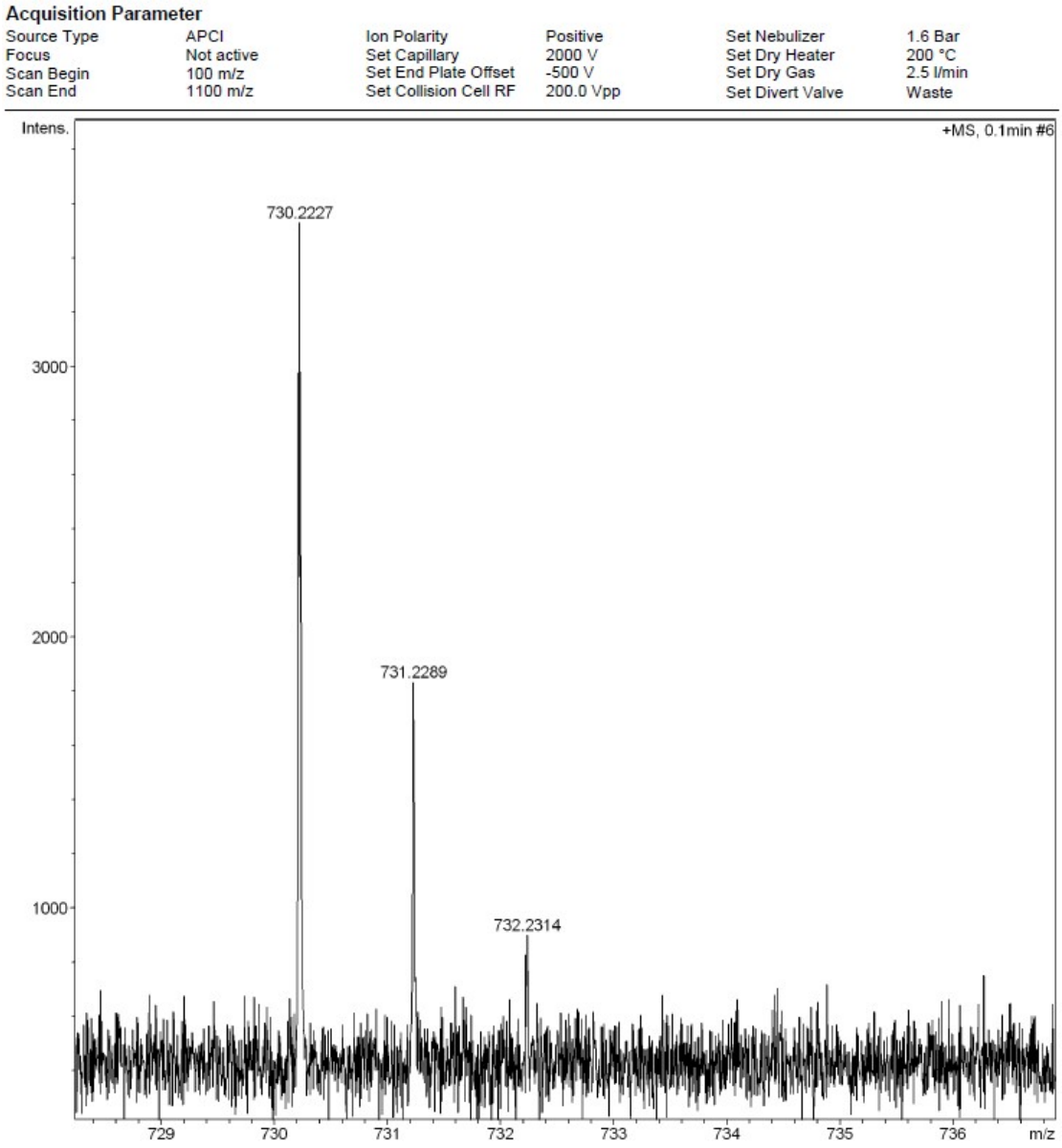

Figure S12. HRMS (APCI) of **dbfTPAAP** in MeOH.

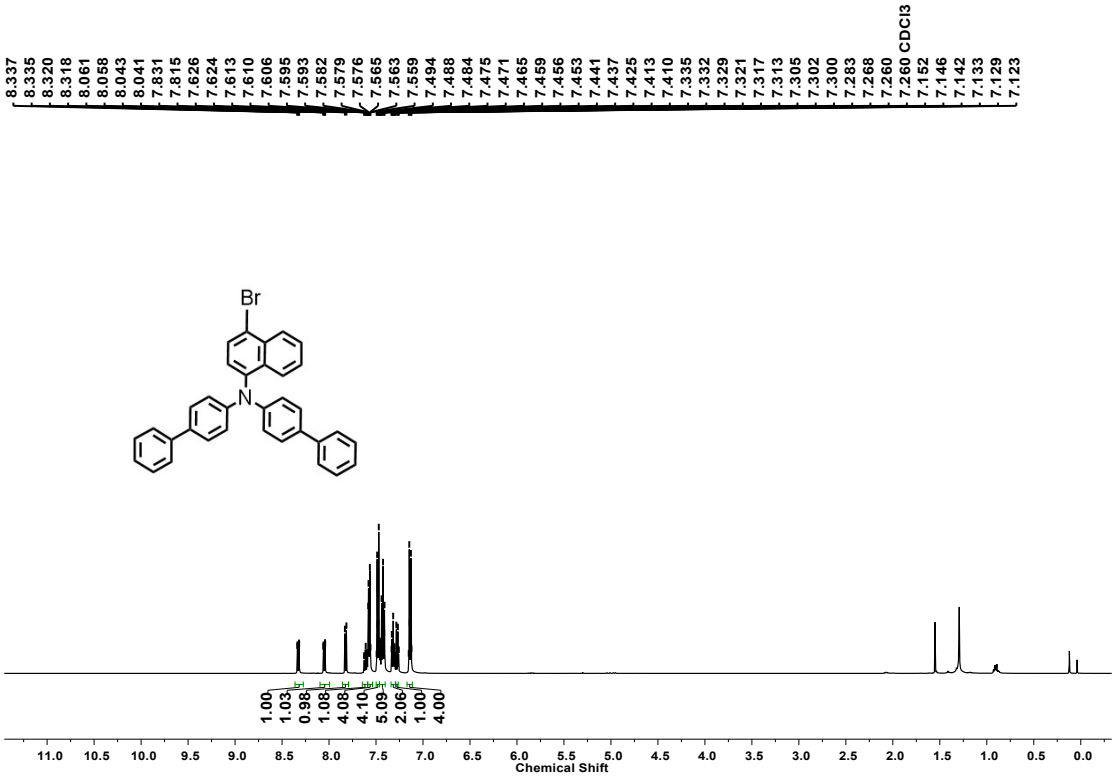

Figure S13. ^{1}H NMR of **B1** in $CDCl_3$.

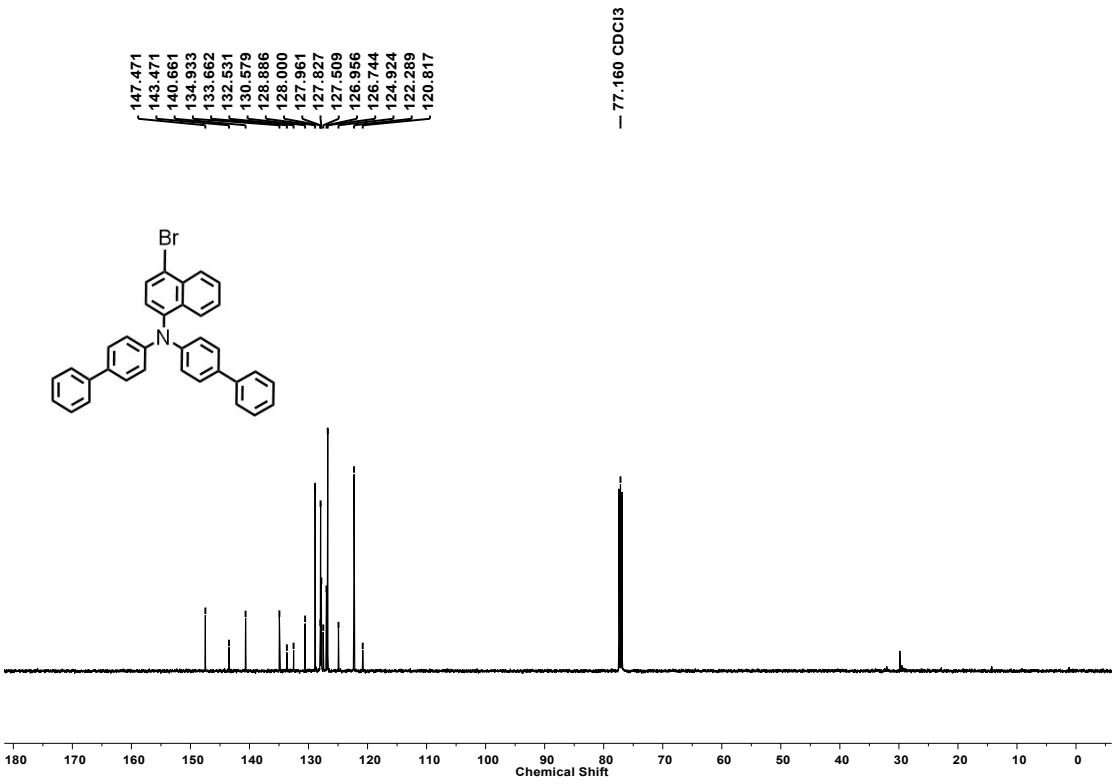

Figure S14. ^{13}C NMR of **B1** in $CDCl_3$.

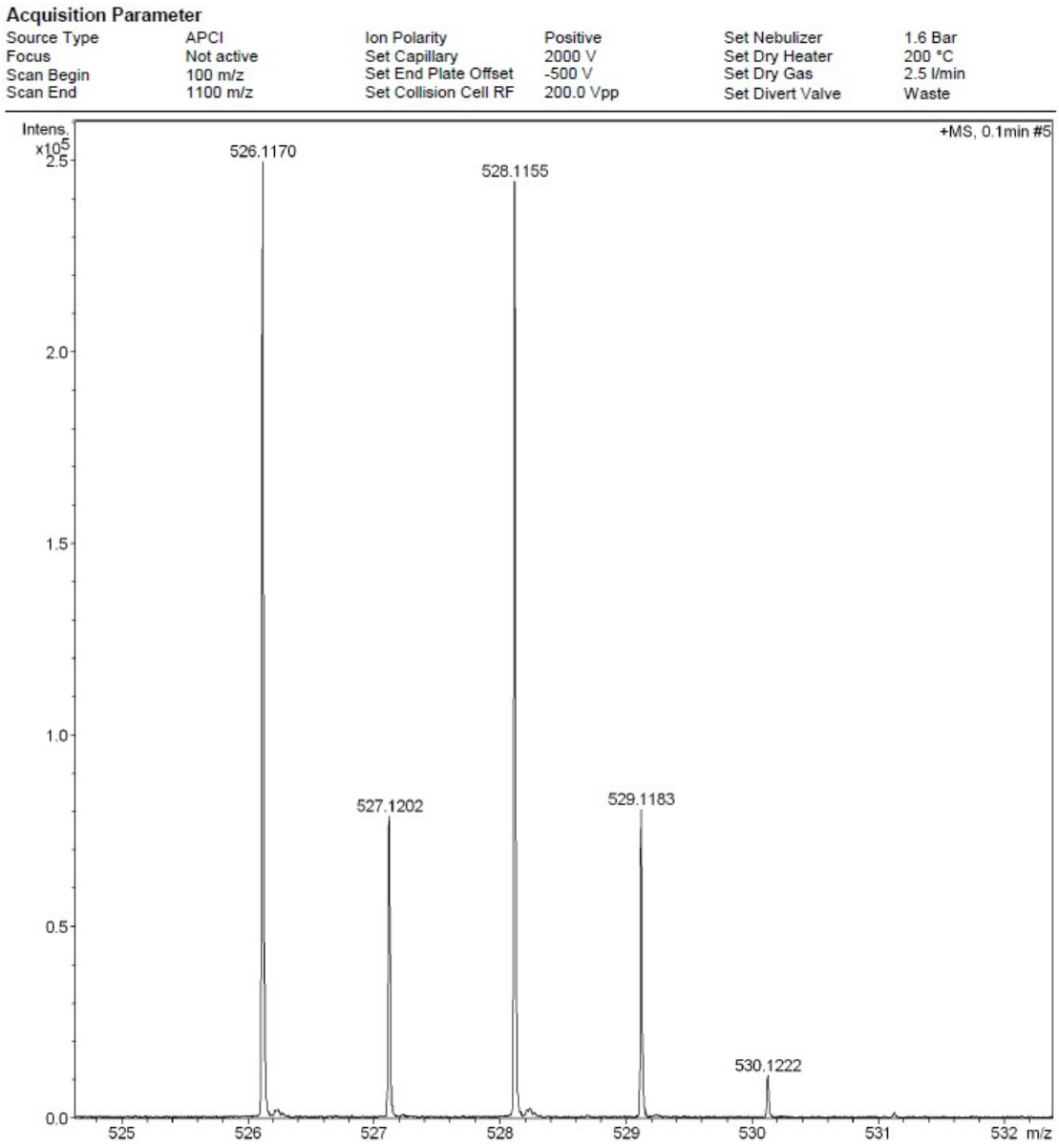

Figure S15. HRMS (APCI) of **B1** in MeOH.

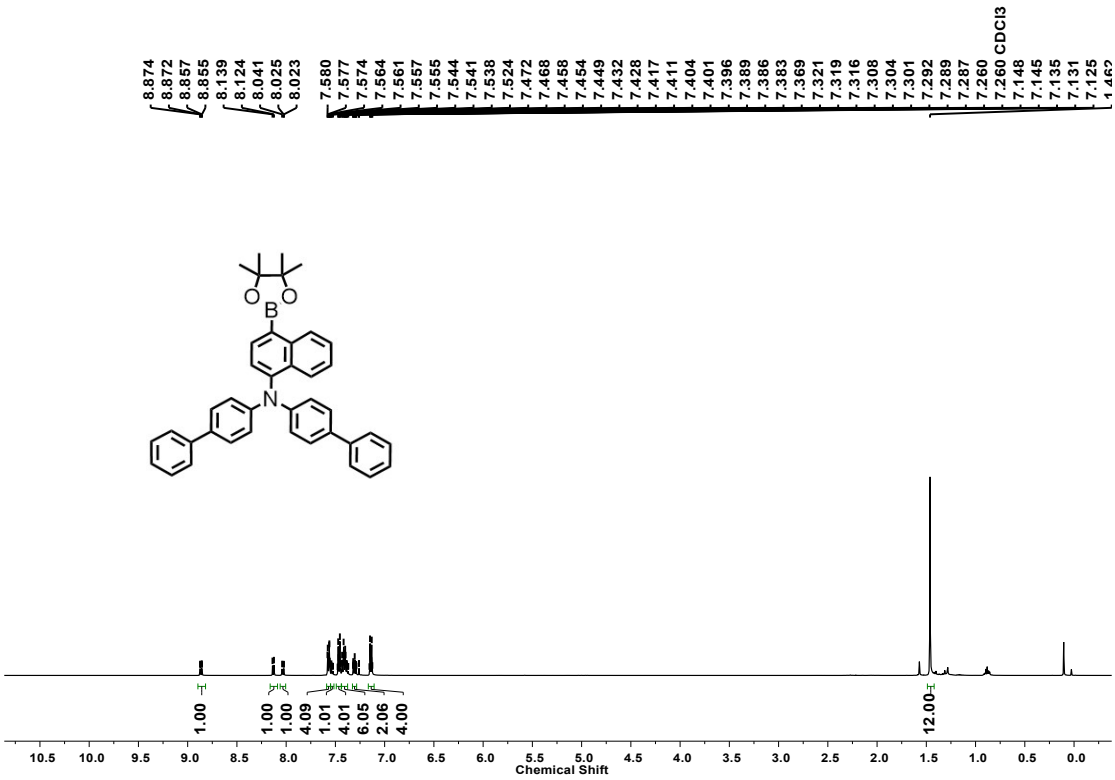

Figure S16. ^{1}H NMR of **B2** in $CDCl_3$.

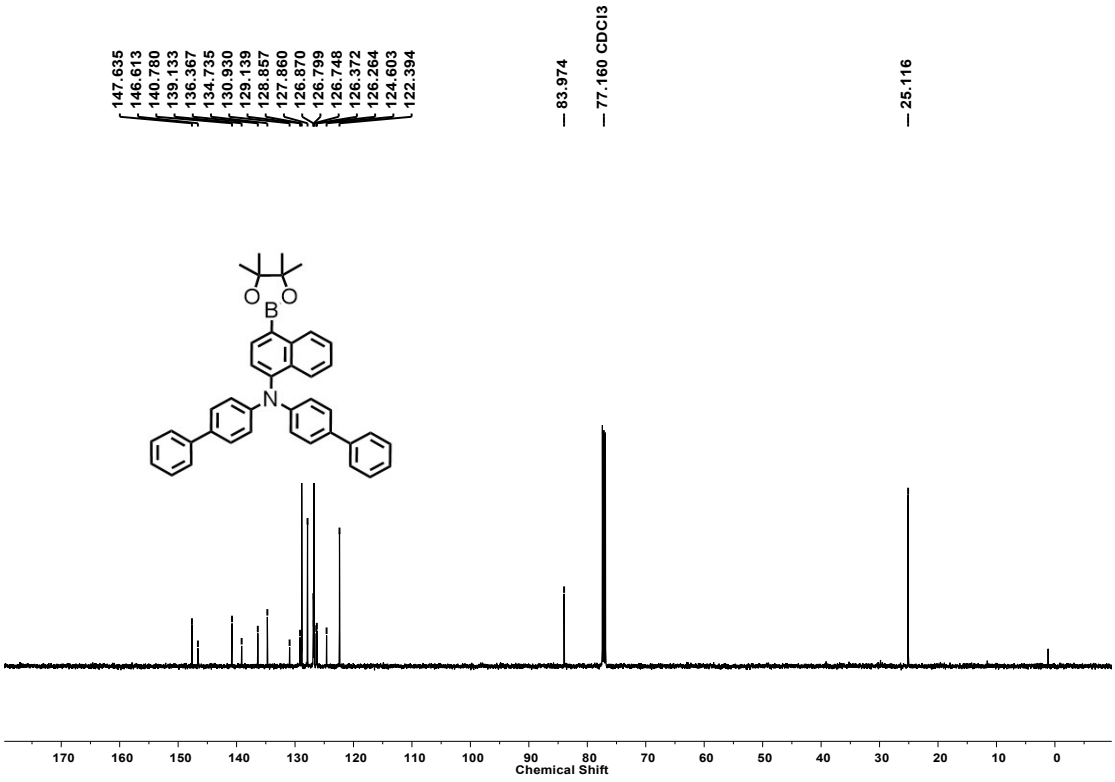

Figure S17. ^{13}C NMR of **B2** in $CDCl_3$.

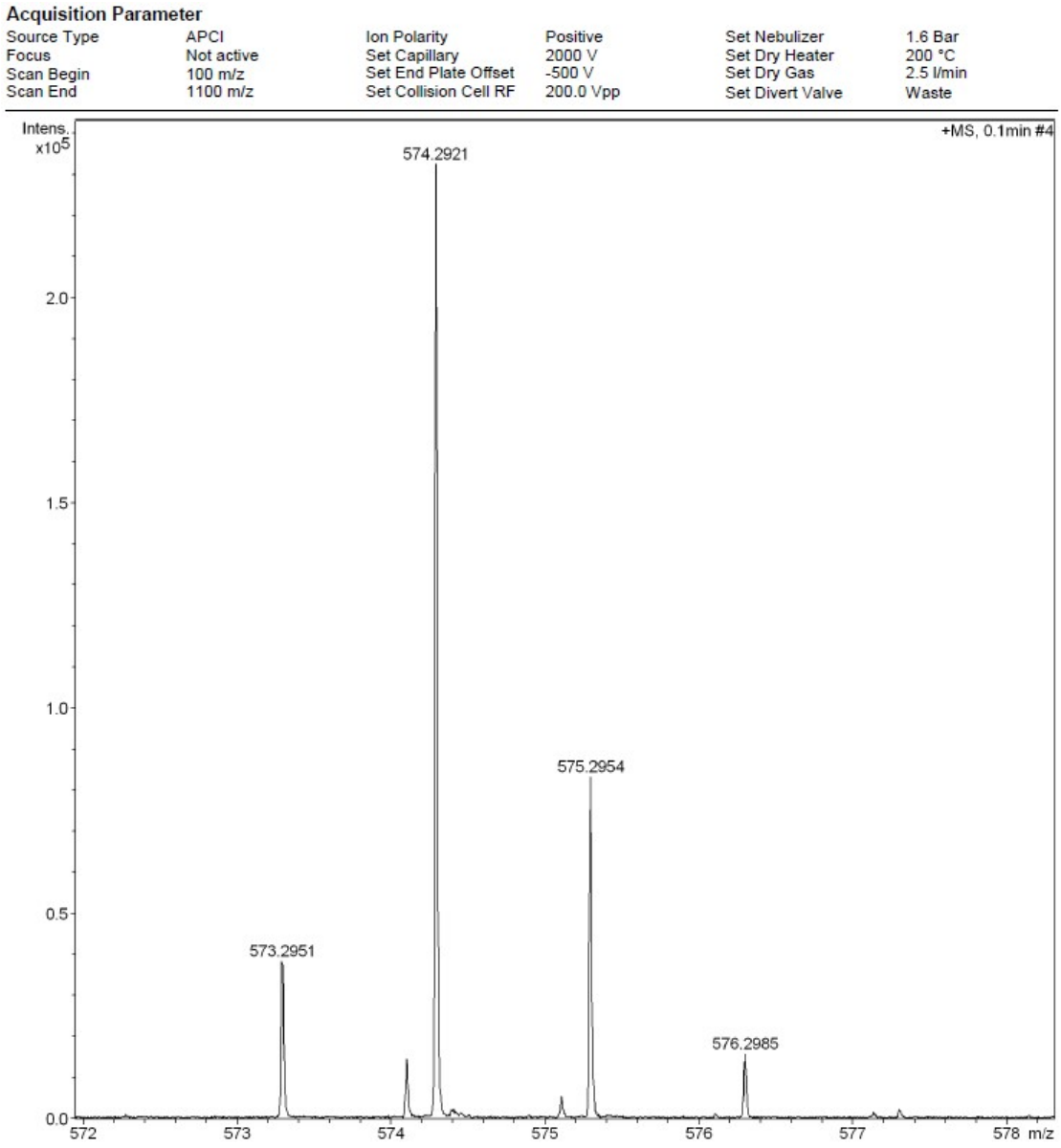

Figure S18. HRMS (APCI) of **B2** in MeOH.

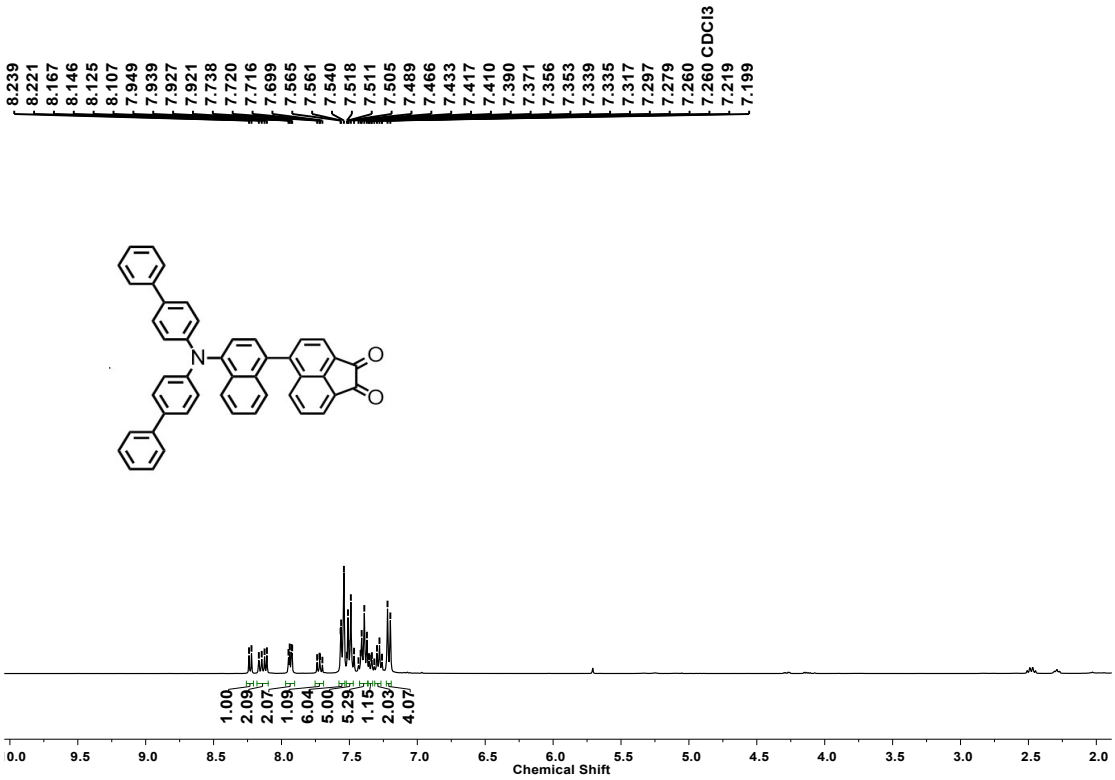

Figure S19. ^{1}H NMR of **B3** in $CDCl_3$.

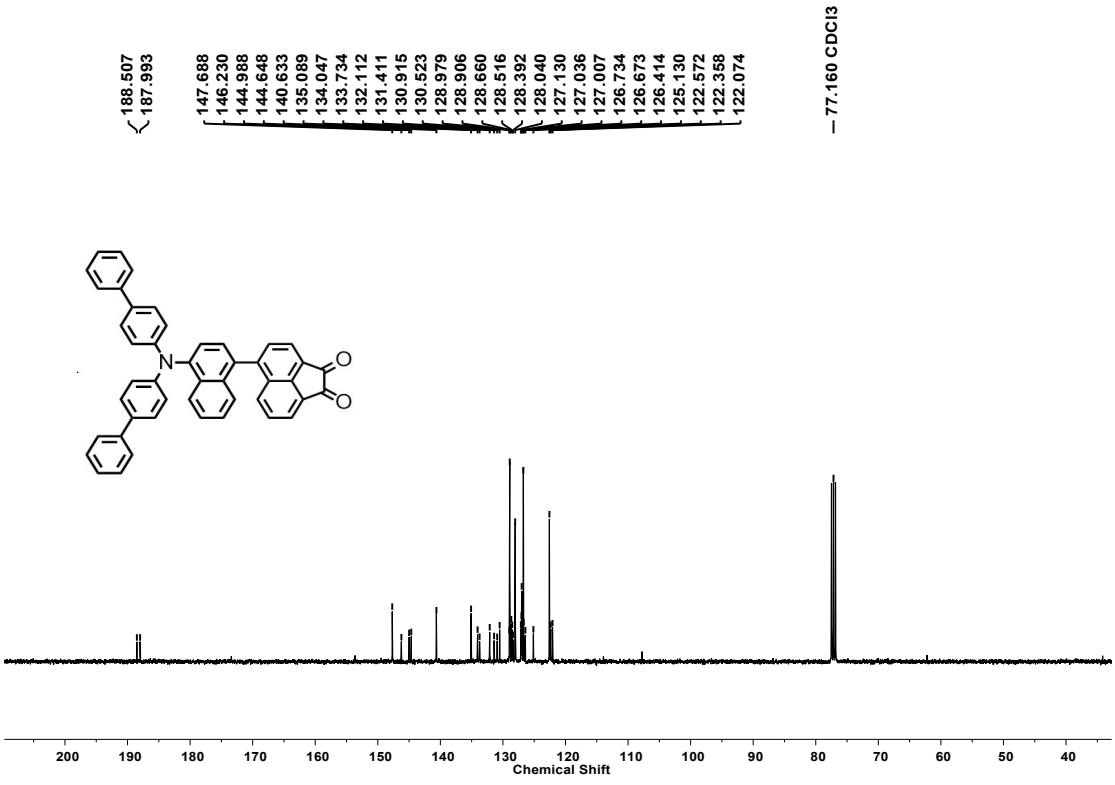

Figure S20. ^{13}C NMR of **B3** in $CDCl_3$.

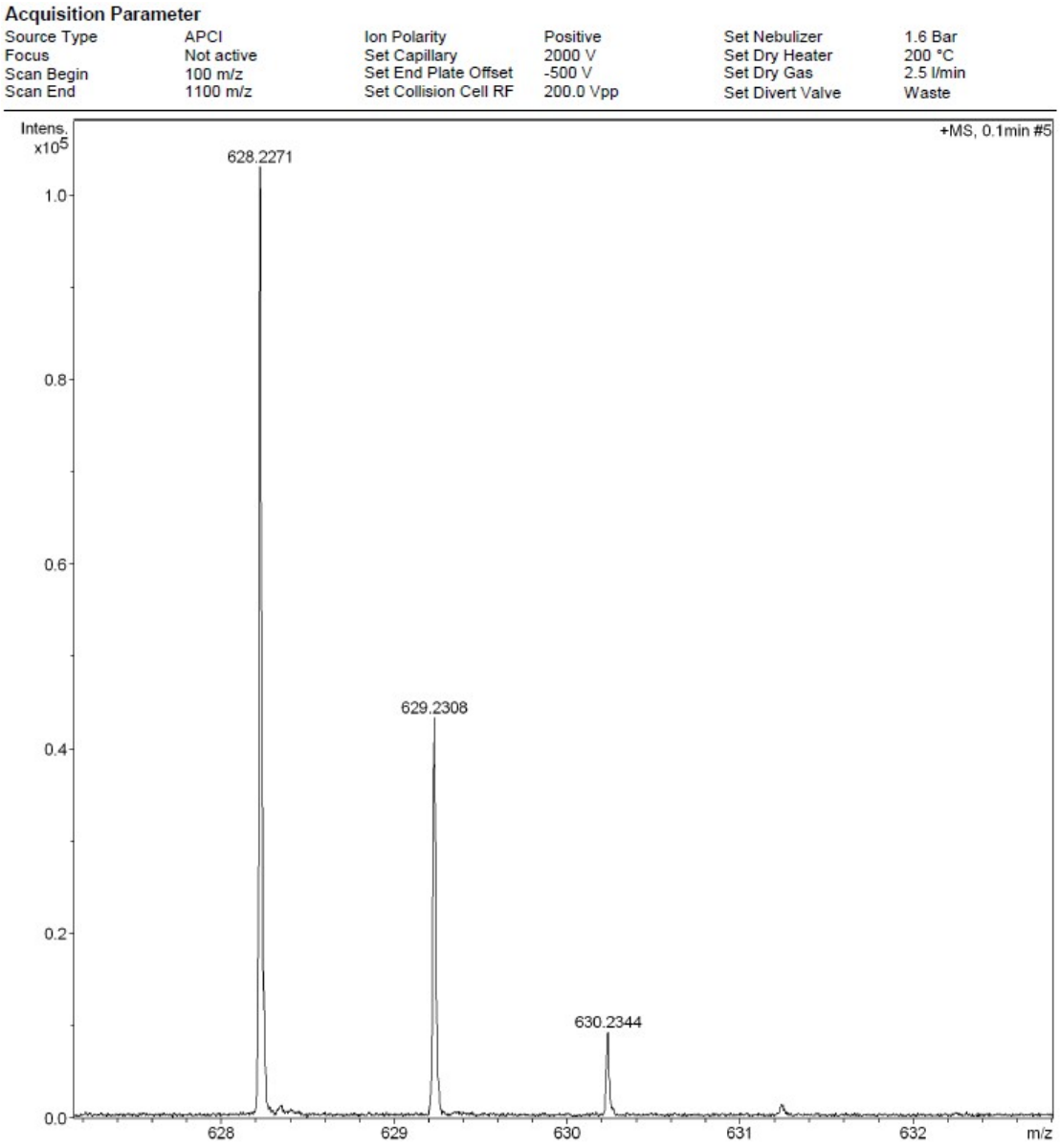

Figure S21. HRMS (APCI) of **B3** in MeOH.

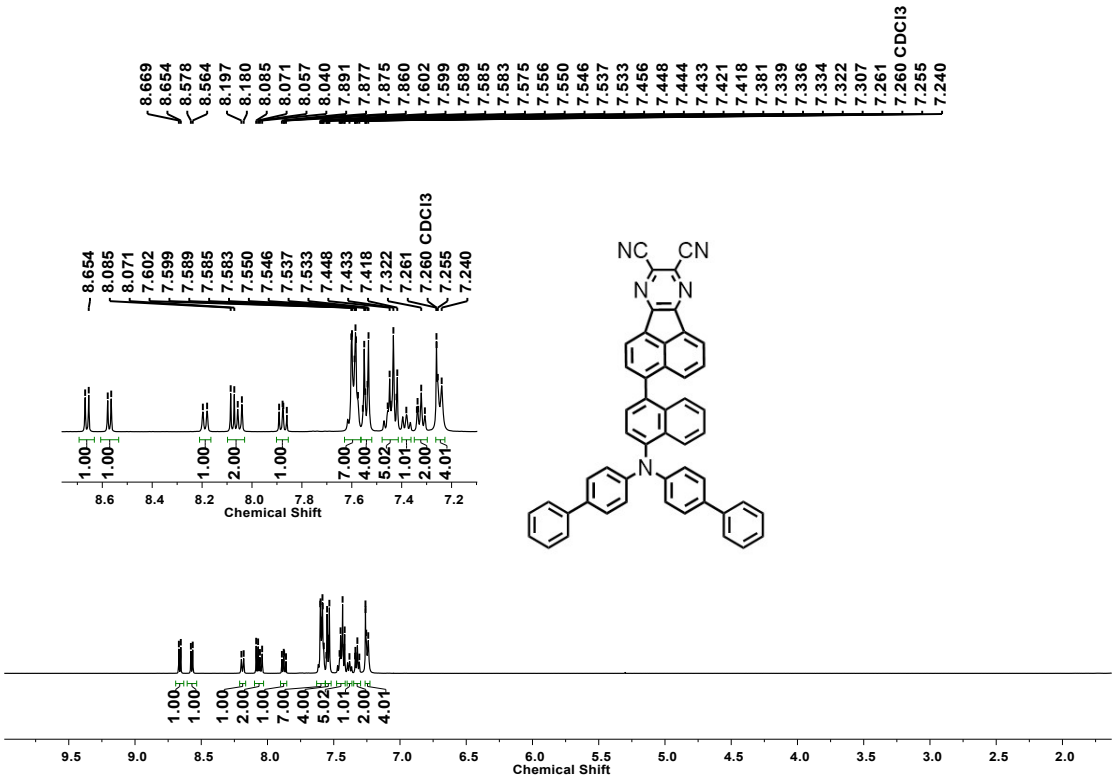

Figure S22. ^{1}H NMR of **dpnTPAAP** in $CDCl_3$.

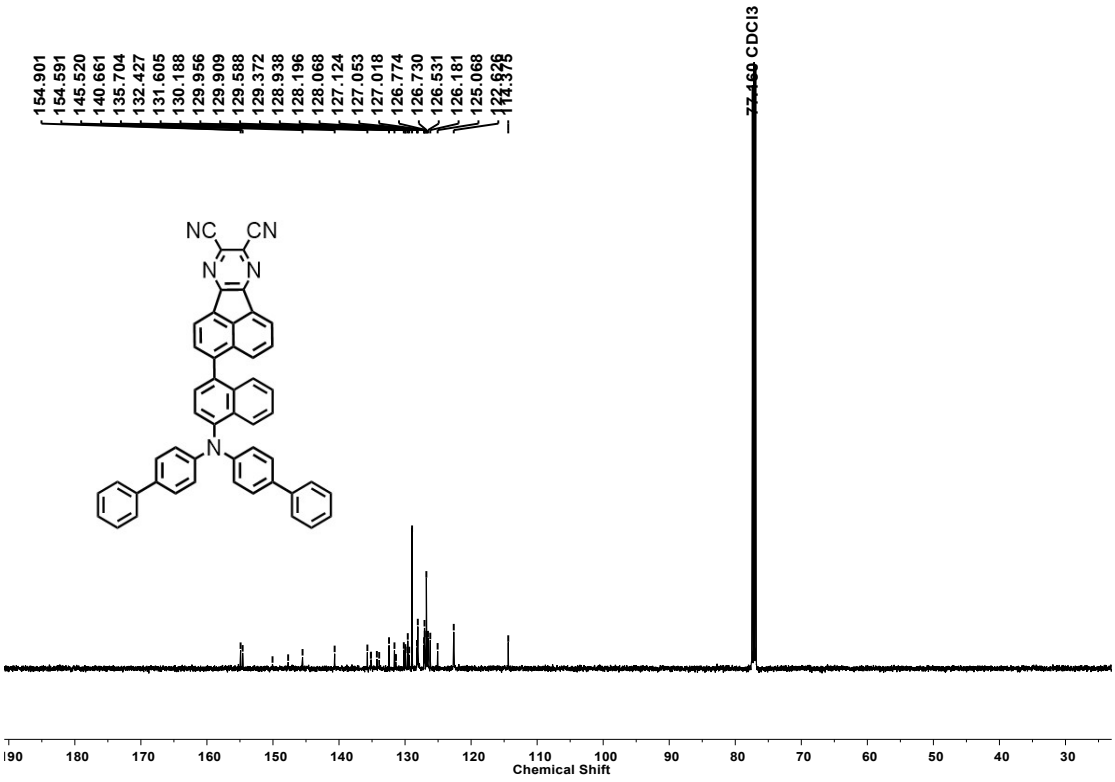

Figure S23. ^{13}C NMR of **dpnTPAAP** in $CDCl_3$.

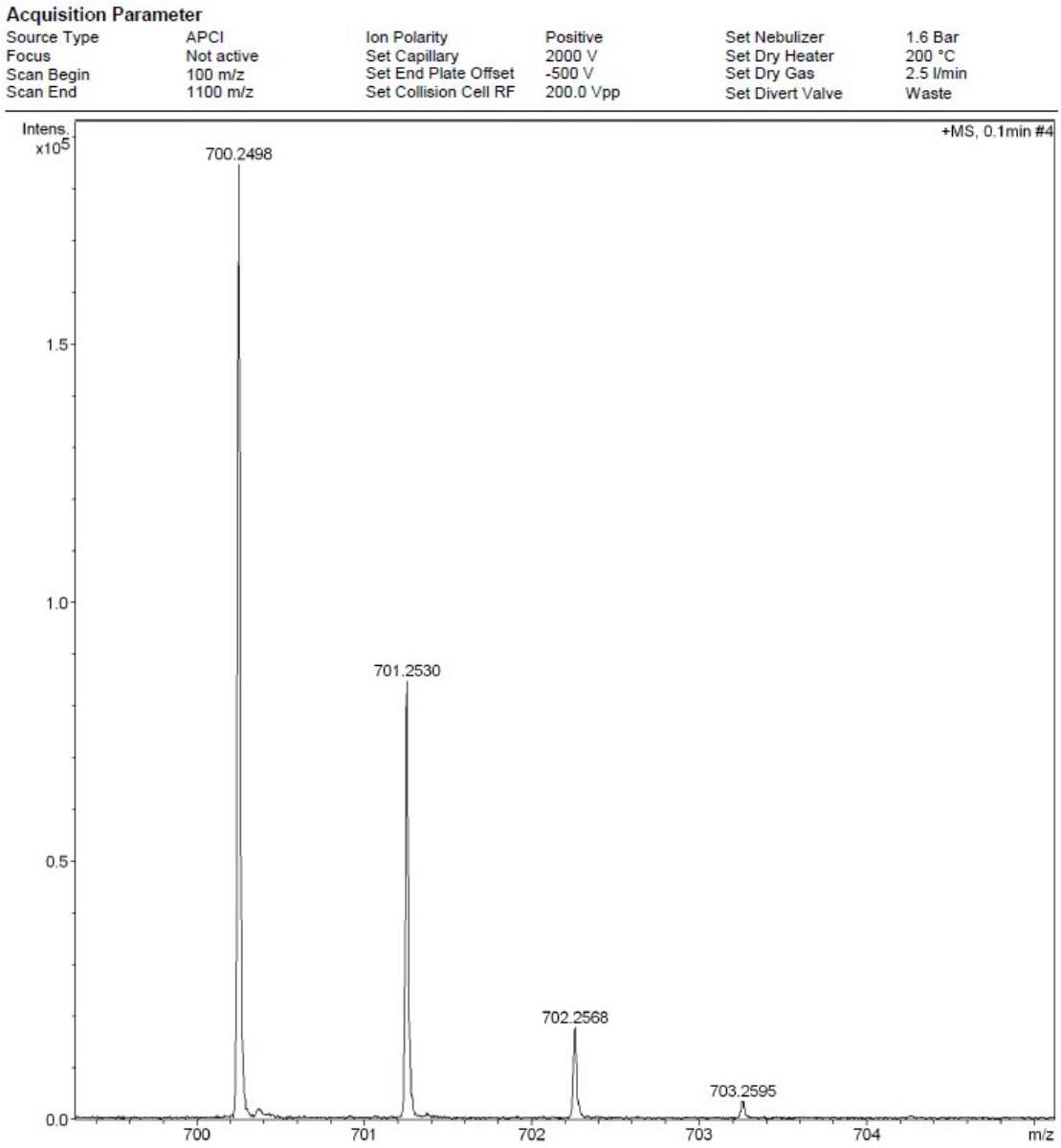

Figure S24. HRMS (APCI) of **dpnTPAAP** in MeOH.

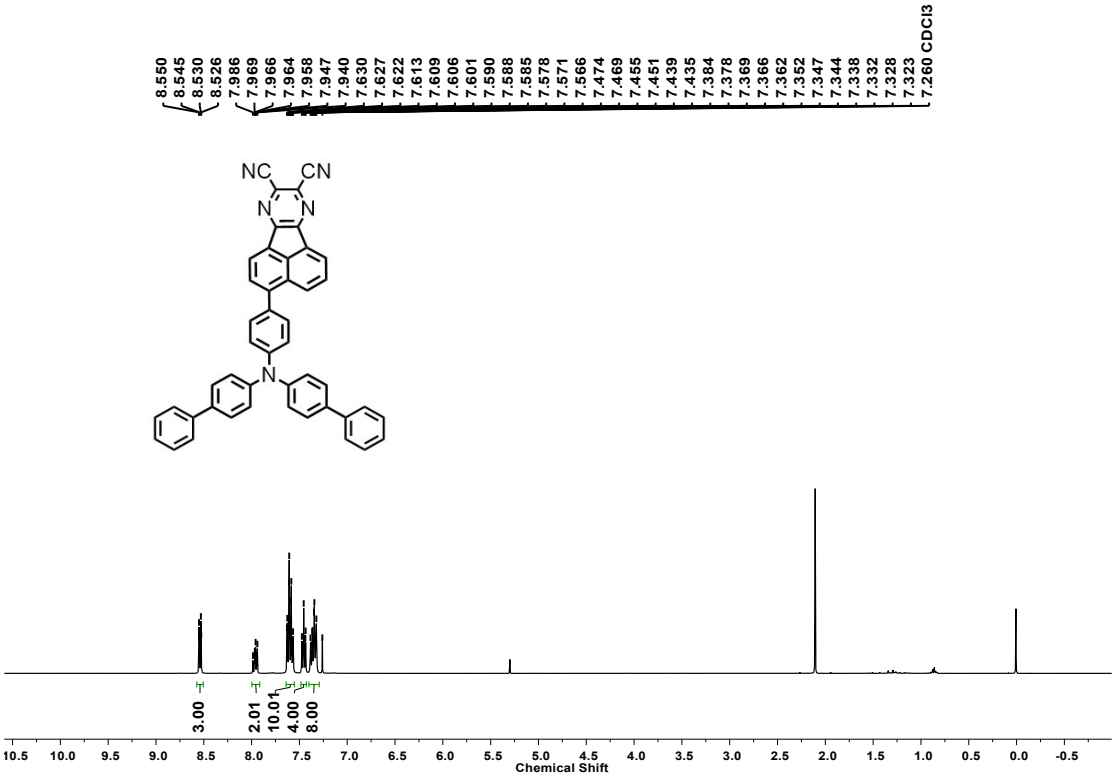

Figure S25. ^{1}H NMR of **dpTPAAP** in $CDCl_3$.

Theoretical calculations

Molecules	dpTPAAP	dbfTPAAP	dpnTPAAP
LUMO	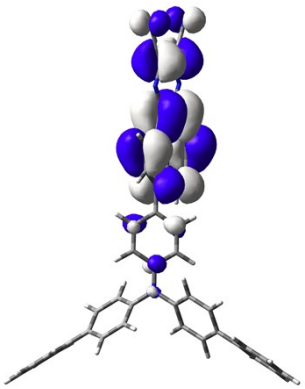	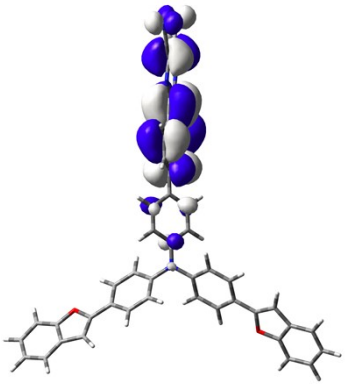	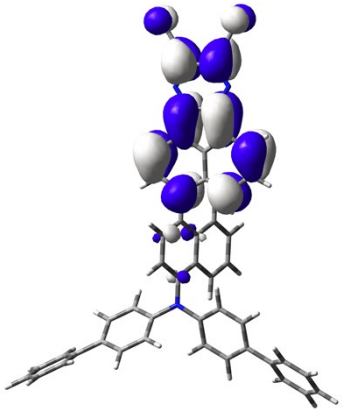
	-3.24 eV	-3.29 eV	-3.32 eV
HOMO	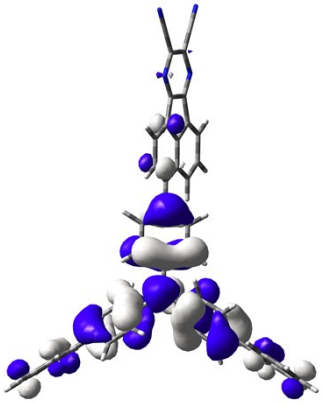	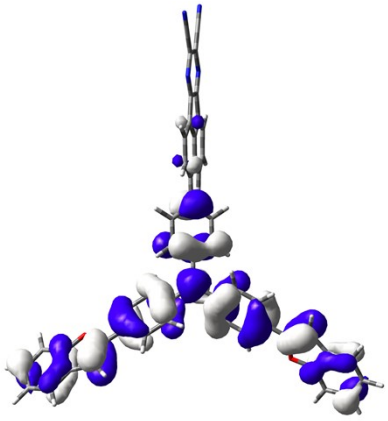	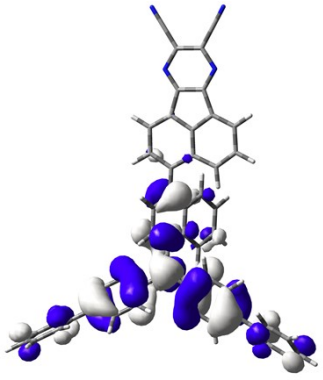
	-5.48 eV	-5.41 eV	-5.43 eV

Figure S26. Visualization diagram of the highest occupied molecular orbitals (HOMOs) and the lowest unoccupied molecular orbitals (LUMOs) of the investigated molecules.

Table S1. Crystal data and structure refinement for **dbfTPAAP**.

Identification code	063063_0m
Empirical formula	$C_{50}H_{27}N_5O_2$
CCDC No.	2184275
Formula weight	729.76
Temperature/K	170
Crystal system	monoclinic
Space group	$P2_1/n$
a/Å	10.5206(17)
b/Å	10.0672(14)
c/Å	34.605(4)
α/°	90
β/°	94.273(5)
γ/°	90
Volume/Å^3	3655.0(9)
Z	4
ρ_{calc}g/cm^3	1.326
μ/mm^{-1}	0.083
F(000)	1512.0
Crystal size/mm^3	0.19 × 0.08 × 0.05
Radiation	MoKα (λ = 0.71073)
2Θ range for data collection/°	3.972 to 49.424
Index ranges	$-12 \leq h \leq 11$, $-11 \leq k \leq 11$, $-40 \leq l \leq 40$
Reflections collected	22050
Independent reflections	6216 [R_{int} = 0.1479, R_{sigma} = 0.1579]
Data/restraints/parameters	6216/0/514
Goodness-of-fit on F^2	1.020
Final R indexes [I>=2σ (I)]	R_1 = 0.0754, wR_2 = 0.1327
Final R indexes [all data]	R_1 = 0.2004, wR_2 = 0.1854
Largest diff. peak/hole / e Å^{-3}	0.29/-0.38

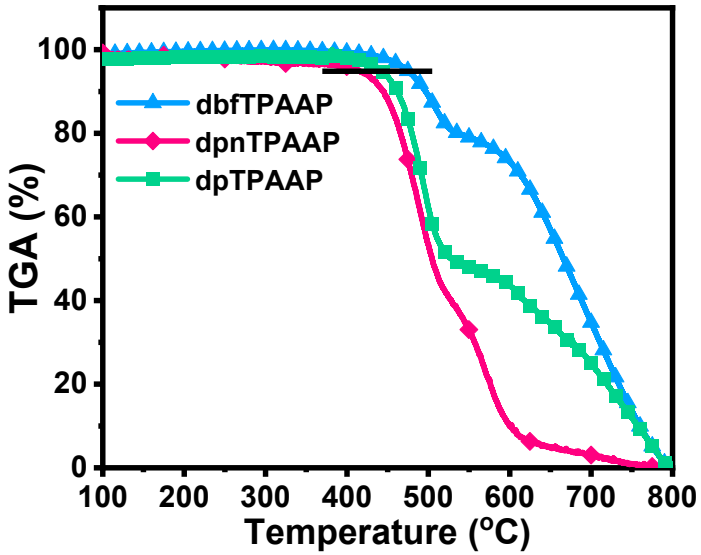

Figure S27. TGA result of **dbfTPAAP** and **dpnTPAAP**, the decomposition temperatures (T_d) of **dbfTPAAP** and **dpnTPAAP** are 480 °C and 425 °C, respectively. **dpTPAAP** was 440 °C.

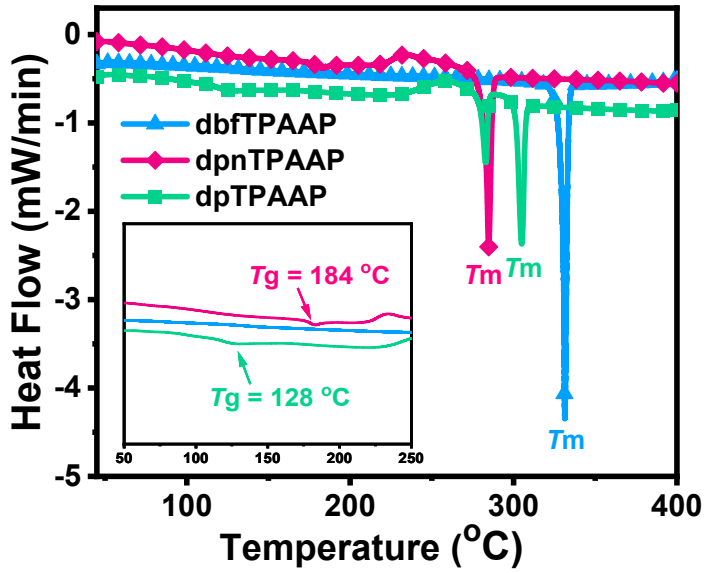

Figure S28. Differential Scanning Calorimetry (DSC) result of **dbfTPAAP**, **dpnTPAAP** and **dpTPAAP**.

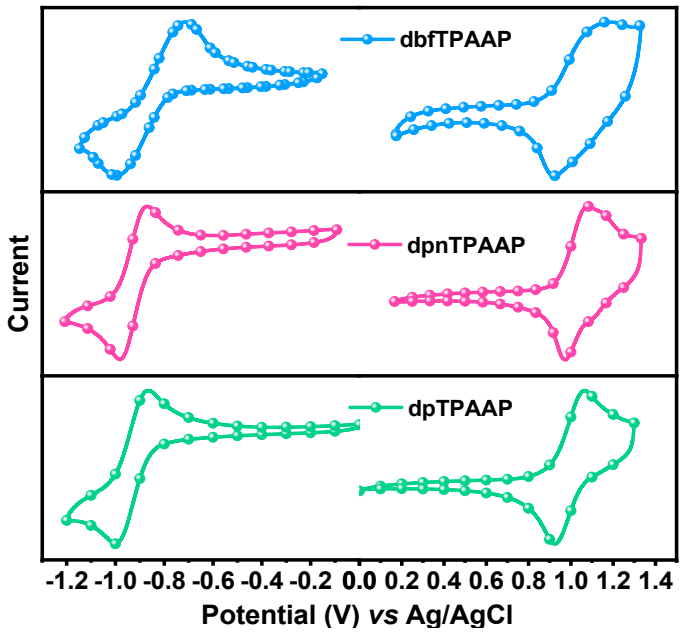

Figure S29. Cyclic voltammetry analysis of **dbfTPAAP**, **dpnTPAAP** and **dpTPAAP**.

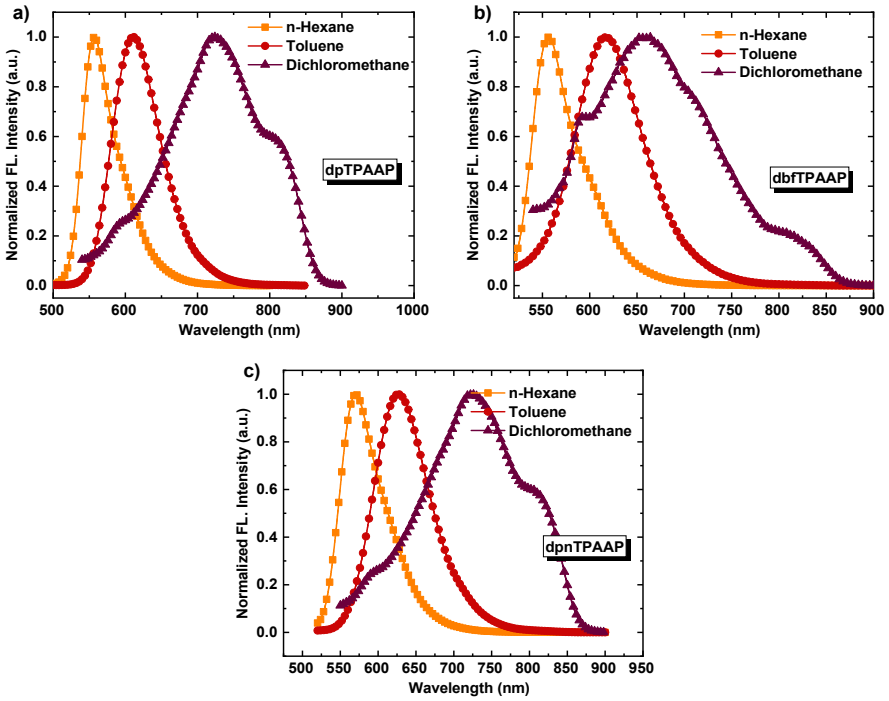

Figure S30. Fluorescence emission spectra in different polarity solvent, a) dpTPAAP, b) dbfTPAAP and c) dpnTPAAP.

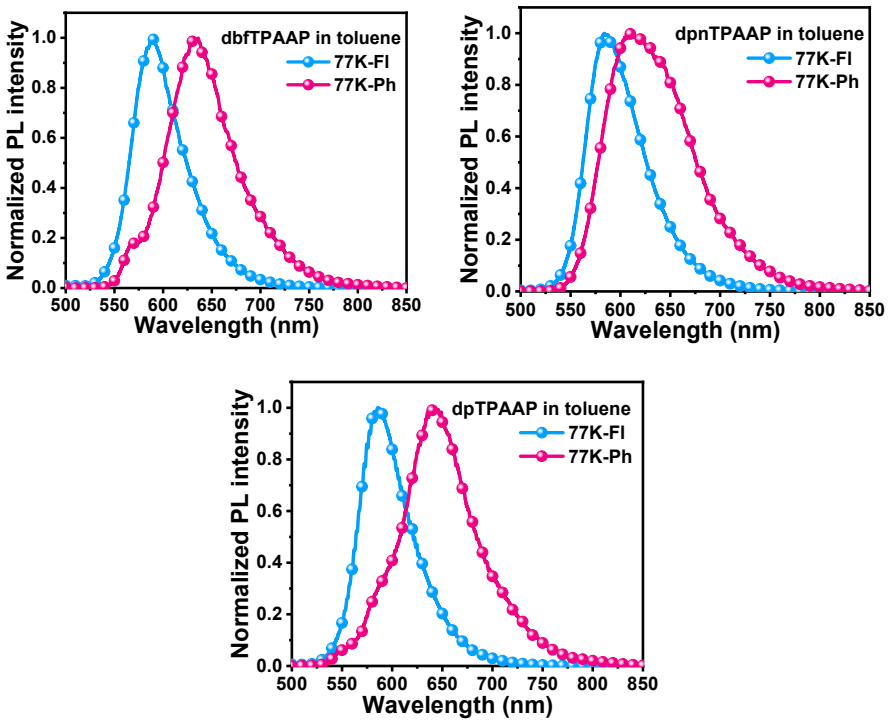

Figure S31. Low-temperature photoluminescence (77K) spectra of **dbfTPAAP**, **dpnTPAAP** and **dpTPAAP** in toluene (10^{-4} mol L^{-1}). The onset energy of LTPL spectra were used to determine the S_1 and T_1 energy level. **dbfTPAAP** (2.26, 2.16), **dpnTPAAP** (2.27, 2.23) and **dpTPAAP** (2.26, 2.12), respectively. The corresponding ΔE_{ST} was measured to be 0.10 eV, 0.04 eV and 0.14 eV.

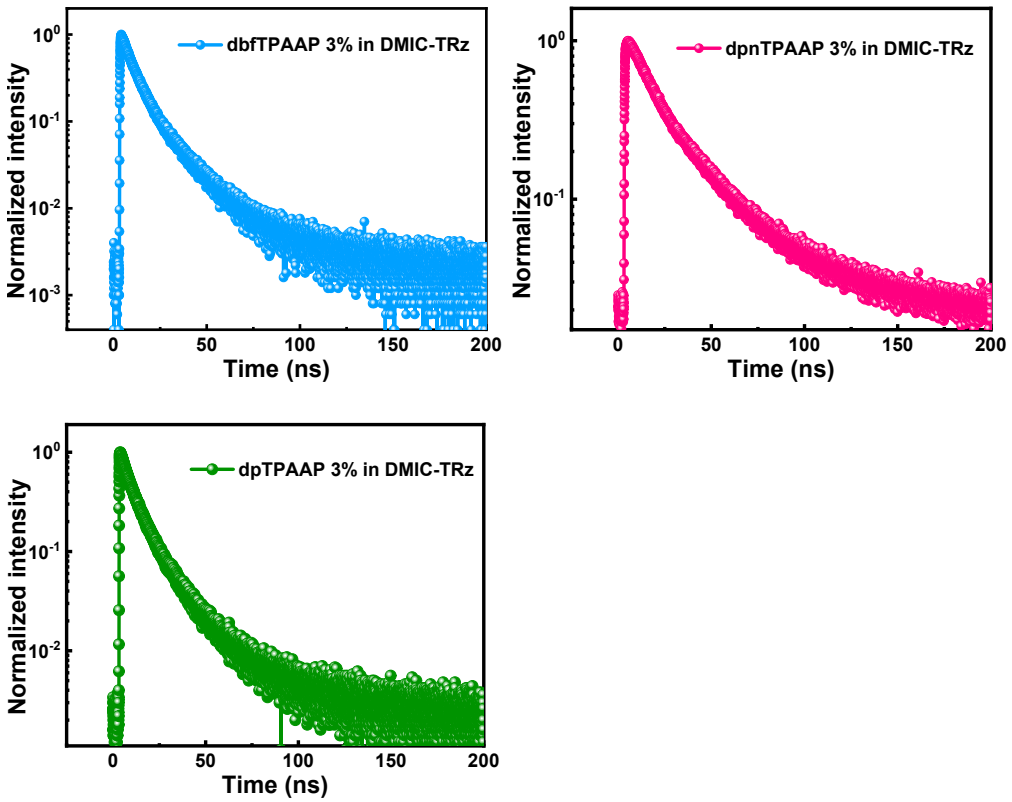

Figure S32. The lifetimes (303K) of the prompt (τ_p) components of the a) **dbfTPAAP**, b) **dpnTPAAP** and c) **dpTPAAP**.

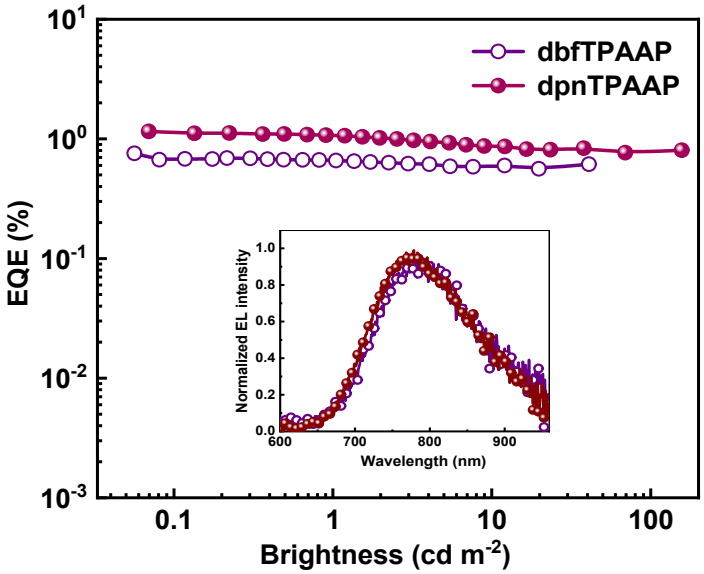

Figure S33. The external quantum efficiency (EQE) *versus* brightness of the two non-doped NIR OLEDs, insert: the EL spectra of the two devices. The devices configuration are "ITO/ HATCN (5 nm)/ TAPC (30 nm)/ TCTA (15 nm)/ mCBP (10 nm)/ dbfTPAAP or dpnTPAAP (30 nm)/ POT2T (20 nm)/ ANT-BIZ (30 nm)/ Liq (2 nm)/ Al (100 nm)".

References:

[1] T. Lu & F. Chen, *J. Comput. Chem*. 2012, ***33***, 580-592.

[2] J. Xue, J. Xu, J. Ren, Q. Liang, Q. Ou, R. Wang, Z. Shuai and J. Qiao, *Sci. China. Chem.*, 2021, **64**, 1786-1795.